MODELING OF CANOPY SPECTRAL SIGNATURE RETRIEVABILITY CONSIDERING 3D CANOPY STRUCTURE VARIATIONS

Christoph C. Borel, Siegfried A.W. Gerstl and Scott N. Martens
Los Alamos National Laboratory, MS D 436
Los Alamos, New Mexico 87545, USA

Abstract

Imaging spectrometers have the potential to be very useful in remote sensing of canopy chemistry constituents such as nitrogen and lignin. In this study, the question of how leaf chemical composition, which is reflected in leaf spectral features in leaf reflectance and transmittance, is affected by canopy architecture was investigated study under the HIRIS project. Several plants were modeled with high fidelity and a radiosity model was used to compute the canopy spectral signature over the visible and near infrared. Model calculations are compared to ground and airborne canopy reflectance measurements. We found that chemical constituent specific signatures such as absorptions are preserved and in the case of low absorption are actually enhanced. For moderately dense canopies the amount of a constituent depends also on the total leaf area.

1 Introduction

The HIRIS team spent the last two years on a study called : "Accelerated Canopy Chemistry Program". The overall goal was to see if a hyperspectral instrument could be used to determine the leaf chemical content (e.g. nitrogen, cellulose, ...). Our task was to investigate how the canopy architecture might change the leaf chemical signature and by how much. Furthermore, we were asked to investigate effects due to illumination, background and terrain on the spectral signatures.

Why is a change in the canopy chemistry signature expected? Since a canopy is a three-dimensional structure of leaves/needles, stems, branches, etc., the radiation emitted from any single phytoelement will interact with many others before it leaves the canopy. Such multiple reflections and transmissions modify the originally emitted leaf spectrum. This conclusion becomes intuitively clear when it is realized that all phytoelements (say leaves) in a canopy structure fall into 3 categories: fully illuminated, fully shaded, or partially shaded/illuminated by the incoming solar radiation; and it is obvious that a shadow spectrum is different from a sun-lit leaf spectrum. Thus, the magnitude of such spectral changes will depend on the canopy architecture and the external illumination direction.

The paper is organized into six parts. First, we review existing canopy models and rated them on what their advantages and disadvantages in this application might be. Second, we list modeling requirements at the leaf, canopy and landscape level. Third, we describe a method for reconstructing trees from geometrical measurements of data on tree geometry for walnut trees, douglas fir seedlings and maple seedlings. We investigate how an absorption feature in a plate is changed if the plate is part of a layered canopy. Fourth, we develop a stacked leaf radiosity model which is compared to measured spectra of stacked aspen leaves. A weighted version of the the stacked leaf model is then applied to the maple seedling canopy. The previously published N-layer model is then used to show how an absorption feature in a plate is changed if the plate is part of a layered canopy. Fifth, we develop a fast hybrid raytracing/radiosity method to compute canopy spectral signatures for variable LAI, view angles and sun angles and compare the results to measurements obtained by AVIRIS over a walnut orchard. Sixth, some conclusions are drawn from the model results.

2 Modeling Requirements

2.1 Leaf Level Reflectance Models

A comprehensive leaf model which relates the spectral signature to leaf chemical composition needs to be adopted or developed. This is however a very difficult task that has not been realized. The best model we know and was available to us to model leaf level reflectances is the PROSPECT model by Jacquemoud and Baret (1990) The model computes leaf reflectance and transmittance as a function of water content in $[cm]$, chlorophyll pigment a+b concentration in $[\mu g cm^{-2}]$ and uses a structural parameter for different types of leaves and their state (green or senescent).

2.2 Soil Reflectance Models

Many canopies do not fully cover the soil surface. Spectral characteristics of the soil background are measured by an imaging spectrometer and must be modeled as well. Jacquemod and Baret (1992 have developed a spectral soil model called SOILSPEC that includes 26 different types of soil and is able to compute soil BRDF's using the Hapke model (Hapke (1981)).

2.3 Canopy Reflectance Models

Many models exist to compute the spectral bi-directional reflectance distribution function (BRDF) of simple plant canopies. Most models however are derived from radiative transfer which requires a conversion from the discrete nature of plant canopies into a volume - averaged model. Thus these models cannot take into account shading or leaf to leaf radiative interactions. In Gerstl and Borel (1992) we give a detailed description of the differences between radiative transfer and radiosity models.

The advantage of RT based analytic models, such as the Pinty-Verstraete (1989) model which is based on Hapke's model, are that solutions can be computed very rapidly and only a few parameters are necessary. The disadvantage is that some of the parameters are very difficult to obtain from canopy geometry measurements.

We believe that the following features are necessary for a canopy model to simulate the spectral signatures at the canopy level :

1. Represent discrete phytoelements (leaves, needles, stems, fruits, etc.) with specified size, location, orientation, reflectance and transmittance.
2. Include transmission and multiple reflections between leaves must be taken into account.
3. Allow direct and indirect illumination.
4. Consider shadowing within the canopy and on the ground.
5. Allow calculation at any wavelength with spectrum transfers between leaves.

Of all the models we are familiar with, only the recently developed radiosity method (Gerstl and Borel (1990), Borel, Gerstl and Powers (1991), Goel et al. (1991), Gerstl and Borel (1992), and Borel and Gerstl (1993)) meets all of the above features.

2.4 Sensitivity Analysis of Canopy Chemistry Signatures

The measured spectral radiance at the sensor level depends on many parameters :

1. Atmospheric conditions
2. Sun / View geometry

3. Sensor characteristics, such as spectral and spatial resolution
4. Terrain effects
5. Canopy spectral BRDF which in turn depends on canopy chemistry and canopy architecture.

The goals of that sensitivity analysis are to :

1. Quantify the sensitivity of the canopy spectral BRDF with respect to relevant canopy architecture parameters (such as leaf area density, tree height and spacing, etc.) and background (soil, litter).
2. Quantify the sensitivity of the canopy spectral BRDF with respect to the canopy chemistry (C/N ratios, Lignin and Nitrogen content, etc) of the phytoelements.
3. Quantify the sensitivity of the measured spectral radiance as a function of atmospheric parameters (optical depth, aerosol scattering phase function, etc.), Sun / View geometry and terrain effects.

2.5 Requirements for Canopy Reconstructions

In order to reconstruct the tree geometry, selected measurements must be performed at the site, vegetation, tree/stem and leaf/needle level. We estimate the difficulty of measurement with numbers from 0=easiest to 10=most difficult. The priority of having them measured for our models ranges also from 0=least important to 10=most important. We also tried to estimate for the needed accuracy of the measured parameters.

Site Characteristics

1) Slope The slope of the ground landscape level at the site may be measured with a Brunton compass or other inclinometer, or can be estimated with the aid of a topographic map or if available from a high-resolution digital elevation model (DEM).

2) Vegetation Cover Fraction The fraction of vegetation covering an area.

Vegetation Characteristics for Trees

Trunk Diameter : The trunk diameter should be measured at breast height (1.37 m) with a diameter tape or regular meter tape.

Tree Height : Tree height can be measured with an inclinometer (or similar device) and a meter tape when a clear line-of-sight to the tree top can be established.

Crown Shape : The tree crown for each species may be described as a simple geometric shape (e.g. spheroid, or an ellipsoid). The dimensions of this shape can be measured as explained below.

Crown Radii : The length of four radii (from trunk center to outline of crown) can be measured at the four principal compass directions as shown in Fig. 4.

Crown Height : The height of the crown from the lowest part to the top of the tree. The height above ground at which the crown starts should also be noted.

In table 1 the landscape level parameters are summarized.

Figure 1 shows symbolic representations of the above parameters.

Landscape Level Parameters				
Symbol	Parameter	Difficulty	Priority	Accuracy in %
T	Terrain Slope	3	8	10
C	Tree Cover (Tree Area / Total Area)	5	10	10
TD	Tree Density	5	10	10
$\vec{P}$	Tree Position	5	10	10
LAI	Leaf Area Index	8	10	10-30
G	Ground Cover Characterization	7	9	-
d	Tree Diameter	1	5	5-10
h	Tree Height	2	10	5-10
S	Crown Shape (e.g. ellipsoidal, triangular,...)	2	5	-
r_i	Crown Radii in 4 Directions	2	5	5-10
H	Crown Height	2	10	5-20

Table 1: Requirements for landscape parameters for the landscape reconstruction

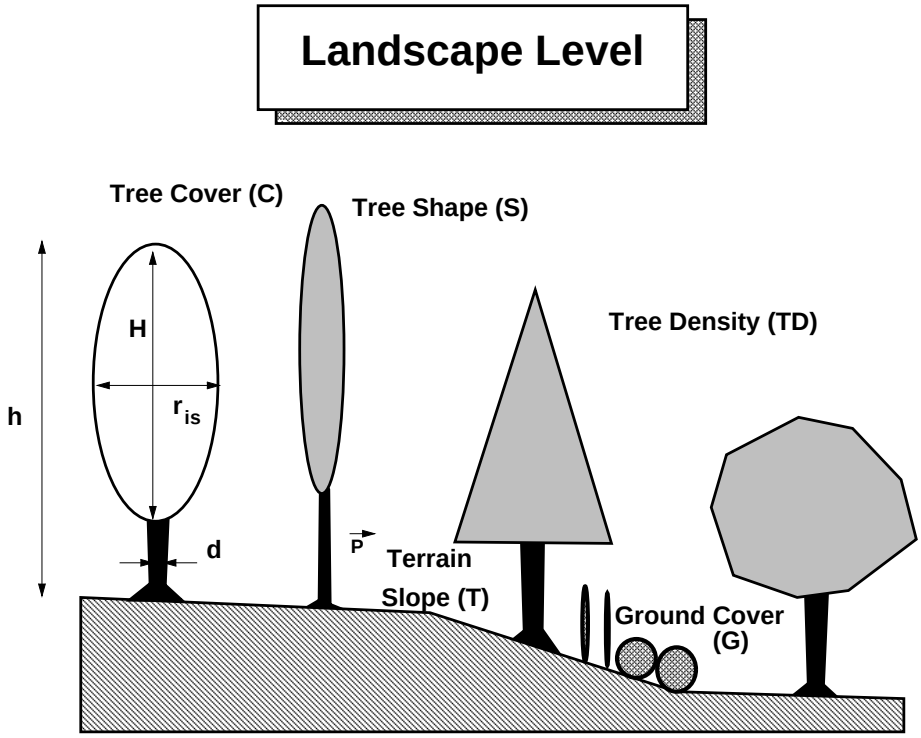

Figure 1: Landscape level parameters

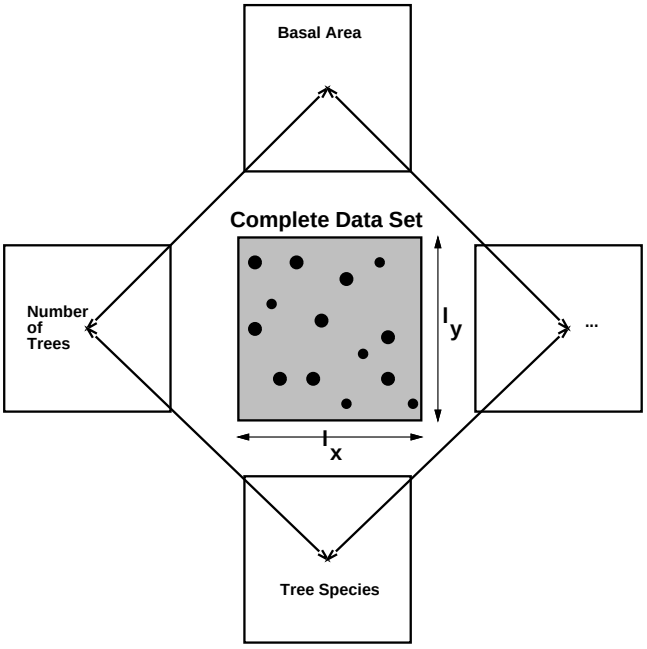

Figure 2: Sampling Strategy

The main goal of the landscape parameters is to establish the heterogeneity of the canopy cover, the mutual shading among trees, and terrain effects. A good sample strategy might incorporate an area where tree positions, tree diameters, crown radii, tree heights and species are known. Some of the parameters such as basal area, tree species composition and tree density could be measured in adjacent plots for confirmation. Figure 2 shows this sampling concept.

Tree positions can be established using triangularization as shown in Fig. 3. Each tree with a diameter exceeding some threshold diameter is labeled. A triangular mesh is laid between trees and the distances measured by using a tape or an ultrasound distance meter.

For each tree the crown radius is measured in four directions as shown in Fig. 4. It would also be helpful to specify the tree species in a mixed forest situation.

High resolution aerial photography would help very much. Tree positions and diameters could be derived from aerial photographs.

Number of Orders of Branching : This characteristic can be determined by visual examination of a tree and simply counting the number of times branching occurs from the trunk to the most smallest stems.

Branching Order of Leaf Bearing Stems : The branching order of stems which bear leaves may be recorded. There are likely to be several orders which bear leaves.

Stem Level Parameters

Stem Diameter : Diameter at the mid-length of a stem may be measured with a ruler.

Stem Length : The length of a stem may be measured with a ruler or tape.

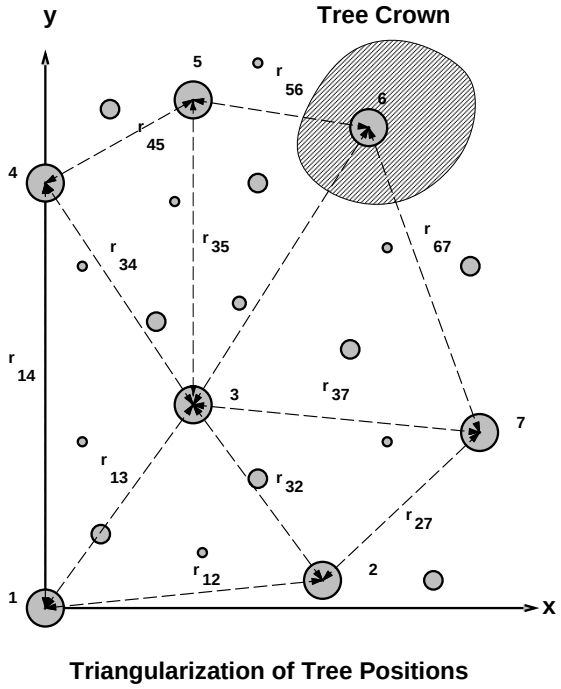

Figure 3: Tree Position Measurement

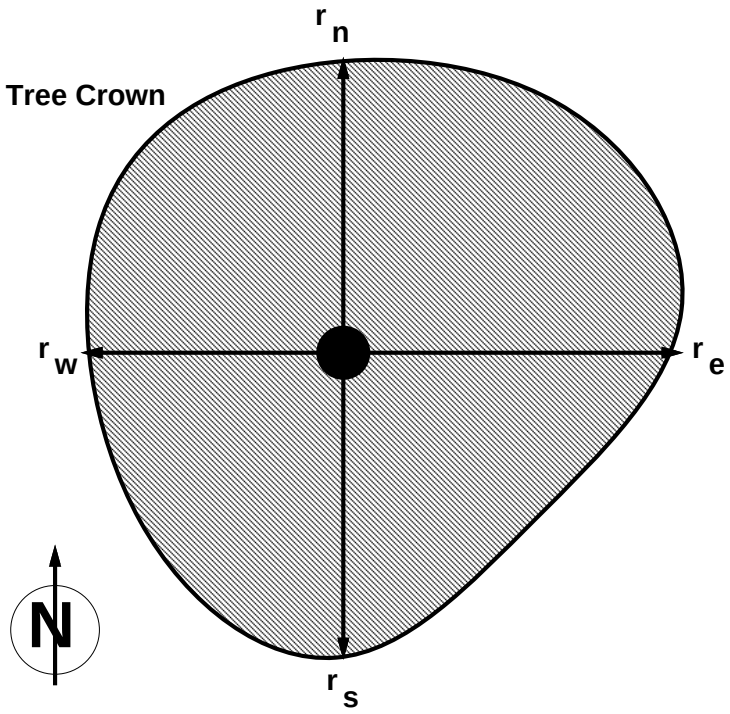

Figure 4: Crown Diameter Measurement

Tree/Stem Level Parameters				
Symbol	Parameter	Difficulty	Priority	Accuracy
n	Number of Orders of Branching	5	7	1-2
N	Branching Order of Leaf Bearing Stems	5	7	1-2
D	Trunk / Stem Diameter	2	4	10 %
l	Trunk / Stem Length Statistics	3	7	10 %
NL	Average Number of Leaves or Needle Whorls per Unit Length	7	6	20 %
θ	Branching Angle	5	8	$5^0 - 10^0$
ϕ	Phyllotaxis Angle	3	7	$5^0 - 10^0$
d	Distance between branching Levels	4	7	5 %
θ_{stem}	Stem Zenith Angle	8	5	$5^0 - 10^0$
ϕ_{stem}	Stem Azimuth Angle	8	5	$5^0 - 10^0$

Table 2: Requirements for tree and stem level parameters for the tree reconstruction

Number of Leaves per unit Length of Stem : For leaf bearing stems, the number of leaves (or needle fascicles) can be counted so that the number of leaves per unit length of leaf bearing stem may be determined.

Branching Angle : The angle of divergence between stems at all orders higher than 1, can be estimated with a protractor.

Phyllotaxis Angle : For coniferous trees (or those with strong monopodial growth), the azimuthal angle of divergence from the main stem can be estimated with the help of a compass.

Table 2 gives a summary of the tree/stem level parameters necessary for the reconstruction of the limb structure.

Leaf/Needle Level Parameters

1. For all Species :

   Leaf Area : One-sided leaf area can be measured on single leaves (or batches if leaves if they are very small, e.g. needles) using a leaf area meter. Alternatively, photocopies of fresh leaves might be used and then later digitized to determine leaf area.

   Leaf Angle Distribution (LAD) : The zenith angle distribution of leaves can be determined most simply by using a protractor to estimate angles. To provide a reasonable distribution more than 50 leaves should be measured.

   Leaf Angle Class Description : The leaf zenith angle distribution can be estimated using standard descriptive terms such as erectophil, plagiophil, spherical, etc.

2. For Broad-Leaved Species :

   Polygon of Leaf Shape : The polygon which describes leaf shape can be most easily determined from photocopies of fresh leaves. Then, the shapes can be easily digitized.

3. For needle-leaved species :

Leaf/Needle Level Parameters				
Symbol	Parameter	Difficulty	Priority	Accuracy
A	Leaf Area	2	8	5 %
L	Leaf Type (single/compound)	1	7	-
LAD	Leaf Angle Distribution	5	7	10 %
LAC	Leaf Angle Class Description (planophil,...)	2	6	-
$\vec{P}_i = (x_i, y_i)$	List of Vectors Describing Leaf/Needle Shape	3	7	5 %
NL	Needle Length Statistic	4	3	10 %
NE	Needle Envelope Description (round,...)	2	3	-

Table 3: Requirements for leaf and needle level parameters for the tree reconstruction

Needle Length : The length of needles may be easily measured with a ruler.

Needle Envelope Description : A geometric solid which describes the volume within which needles along a leaf-bearing stem occur. Examples are boxes, cylinders or ellipsoids. The estimated dimensions of this solid could be given but can also be determined from Needle Length and leaf density.

Table 3 gives a summary of the leaf/needle parameters needed for the reconstruction.

3 Tree Reconstruction

Extensive geometric descriptions of plant canopies are rare, perhaps due to the difficulty of obtaining such data. Hence, many existing models of plant canopy reflectance which are based on radiative transfer theory (e.g. Kimes and Kirchner (1982); Goel and Grier (1988)) use simplistic representations of plant canopy geometry. Even if more geometric data were available these models may not be easily extensible.

Previous attempts to generate realistic trees were based on fractals (Borel (1986,1988)) and Lindenmayer systems (Prusinkiewicz and Lindenmayer (1990); Goel, Knox and Norman (1991)). However it is very difficult to derive the model parameters for these methods. The trees look rather artificial and idealized compared with natural trees that grow under the influence of weather, changing light environments, wind damage and drought conditions.

It is very difficult and time consuming to generate accurate geometric models of natural trees. We have developed a 3-D acoustic digitizer to capture tree geometry accurately and efficiently (R. Schroeder, T. Hornung J. Glas, D.-U. Eisser and U. Gläser (1992-1993)). Unfortunately we have not been able to make any measurements with it yet because of the limited angular coverage of the transducers and microphones used.

Models of canopy reflectance based on radiosity are capable of incorporating significant detail regarding plant canopy geometry (Borel et al. (1991) and Goel et al. (1991)).

A basic description of plant geometry involves locating phytoelements (stems, leaves, fruits) of specified size and shape at appropriate locations in three-dimensional space in their proper geometric orientations. Volumetric representations of plant canopies, often used in modeling do portray the shapes and orientations of phytoelements. However, because of random placement within volumes they fail to properly represent the relative locations of elements as they are in real, nonhomogeneous canopies.

3.1 Walnut Tree and Orchard Reconstruction

A realistic, spatially explicit model of tree canopy structure has been constructed from an existing data set of walnut tree geometry (Martens et al. (1991) and Ustin et al. (1991)). These data include information on the shape, orientation, and spatial location of phytoelements necessary for the complete description of the

Linked List					
Segment Number	Parent Segment	Length in cm	Diam. in cm	Stem Zen.	Stem Azi.
1	0	77	13.9	0	0
2	1	59	6.5	51	180
3	1	192	6.0	45	81
4	1	65	5.0	51	355
5	1	76	11.8	13	345
6	2	20	5.2	55	155
...	...	...	...	...	...

Table 4: Linked list to describe stem structure of a walnut tree

tree canopy. Stem geometry data were collected in a manner which easily allowed graphic representation of the actual branching structure of the measured trees (Martens et al. (1991)). Subsampling the smaller stems in a similar way allowed detailed reconstruction of small portions of canopy. A detailed description of the size, shape, and spatial orientation of the leaflets of the compound leaves was also included.

It is outside the scope of this paper to describe the details of how the field measurements where used to derive statistics on the stems, rachis (stem where leaflets attach) and leaf size and orientation. A paper on this work is in progress (Martens (1992) and Martens and Borel (1994)).

The walnut tree representations were generated from a linked list of stem angles (zenith, azimuth) and stem lengths. An example of a linked list for the tree is given in Table 4.

A hierarchical description of each tree was generated from the linked list by a BASIC program. The hierarchical description is very compact and describes a tree with as few lines as possible. The hierarchical description can also be computationally efficient since a raytracer must test for intersections with potentially every object in the scene. Each object has usually a bounding box, i.e. a region where an intersection is likely, associated with it. By clumping many small objects together (e.g. the polygons and cylinders that make up one leaf) the number of bounding box tests is reduced.

The data output from the model was designed as an input file for the ray-tracing program *Rayshade* in order to graphically render the trees. *Rayshade* is designed to ray-trace scenes designated with primitive geometric solids (e.g. cylinders, spheres, polygons) although more complicated objects can be built using constructive solid geometry. The objects can be rotated, translated, scaled, and surface characteristics may be specified. Lighting and view points are also easily designated.

The public domain raytracer called *Rayshade* is available by FTP from `princeton.edu (128.112.128.1)`. Information on *Rayshade* can be obtained via Mosaic using the Uniform Resource Locator address (URL): `http://www.princeton.edu/grad/cek/rayshade/rayshade.html`.

The stem structure of the tree was specified as consisting of cylinders, each terminating with a sphere (Borel (1988)). The center of the sphere is at the point formed by the center of the cylinder as it intersects the end plane of the cylinder. The spheres fill gaps that would otherwise appear in the rendered image at the junctions of cylinders which have a divergence angle > 0. For example the stems of a tree are described by :

```
/* r3t09p.stm created by RayTree.BAS V3.00   09-09-1992 10:20:03 */
/* from input file: r3t09p.fm2 */
/* Random number seed =  124  */
/* Phyllotaxis Delta angle = 164  */
/* define ground polygon and specify ground color */
applysurf  ambient 0.0500 0.1500 0.0500
```

```
          diffuse 0.2000 0.6000 0.2000
poly
    10000.00  10000.00      0.00
   -10000.00  10000.00      0.00
   -10000.00 -10000.00      0.00
    10000.00 -10000.00      0.00
/* specify stem color */
applysurf  ambient 0.1750 0.1000 0.0500
           diffuse 0.7000 0.4000 0.2000
cylinder  6.95    0.000    0.000    0.000     0.000    0.000   77.000
sphere    6.95    0.000    0.000   77.000
cylinder  3.25    0.000    0.000   77.000     0.000  -11.657   86.440
sphere    3.25    0.000  -11.657   86.440
cylinder  0.30    0.000  -11.657   86.440    -5.235  -14.559   86.858
sphere    0.30   -5.235  -14.559   86.858
cylinder  0.30   -5.235  -14.559   86.858    -5.055  -19.699   89.949
sphere    0.30   -5.055  -19.699   89.949
cylinder  3.25    0.000  -11.657   86.440     0.000  -23.314   95.880
sphere    3.25    0.000  -23.314   95.880
cylinder  0.30    0.000  -23.314   95.880     8.376  -25.403  104.216
.........
```

Leaves were specified hierarchically. Each leaflet consisted of two polygons joined along the midrib whose total outline formed an octagon as previously mentioned. A leaf was composed of the appropriate number of polygons depending on the number of leaflets per leaf. The rachis consisted of a 1.5 mm radius cylinder. The polygons were rotated in space as previously described to achieve the desired geometry as determined by irrigation treatment and rachis zenith. The leaves are then attached to the branches using the following instructions :

```
/* r3t09p.lvs created by RayTree.BAS V3.00   09-09-1992 10:20:03 */
/* from input file: r3t09p.fm2 */
/* Random number seed =  124  */
/* Phyllotaxis Delta angle = 164  */
#include "lvs100.def"
applysurf  ambient 0.0225 0.3250 0.0225
           diffuse 0.1000 0.7000 0.3000
           specular .9 .9 .9
           specpow 3
cylinder  0.15   -5.085  -18.842   89.434    -7.143  -21.318   90.160
object LEAF100_7_120
rotate 1 0 0  335.000
rotate 0 0 1  140.000
scale 0.1 0.1 0.1
translate    -7.143  -21.318   90.160
cylinder  0.15   -5.123  -17.757   88.781    -1.988  -16.767   89.069
object LEAF100_5_170
rotate 1 0 0  285.000
rotate 0 0 1  288.000
scale 0.1 0.1 0.1
translate    -1.988  -16.767   89.069
cylinder  0.15   -5.161  -16.672   88.129    -7.326  -17.887   85.955
```

```
object LEAF100_7_160
rotate 1 0 0  295.000
rotate 0 0 1  119.000
scale 0.1 0.1 0.1
translate    -7.326  -17.887   85.955
cylinder  0.15   24.978  -34.485  115.234    25.990  -33.525  118.225
..........
```

where each compound leaf name contains information on the treatment (33 or 100 % irrigation), number of leaflets (5,7 or 9) and the stem zenith angle (from 50 to 180 degrees in 10 degree steps). A individual compound leaf is made up of a collection of leaflets and a stem represented by a cylinder :

```
/* begin specification of leaf */
name LEAF100_5_80
 list
 cylinder  1.5  0  0  0  0  109.2259  0
 object LAT100_5_1_80_R
 object LAT100_5_1_80_L
 object LAT100_5_2_80_R
 object LAT100_5_2_80_L
 object TERM100_5_80
 end
```

and each leaflet is defined as a scaled, rotated and translated version of a leaf :

```
name LAT100_5_2_80_R
   object LAT100_5_2
   scale -1 -1 1
   rotate 0 1 0  170
   rotate 1 0 0  139.5499
   rotate 0 0 1  90
   translate  1.5   74.08168  0
```

and finally an individual leaf is composed of two polygons that approximate photocopied samples taken from the tree :

```
/* Lateral Lflt: left lflt of pair 2 of  2, 100% ET, poly coords -- in mm */
name LAT100_5_2
list
poly
   0.00000    0.00000    0.00000
  26.90528   32.16243    5.64629
  33.31129   59.56005    6.99065
  27.54587   89.34007    5.78073
   0.00000  122.69370    0.00000
   0.00000    0.00000    0.00000
poly
   0.00000    0.00000    0.00000
   0.00000  122.69370    0.00000
 -16.65565   89.34007    3.49532
 -20.49926   59.56005    4.30194
 -17.29625   32.16243    3.62976
```

```
   0.00000     0.00000     0.00000
end
```

Surfaces of the leaves were assigned to be green (by assigning a mixture of red, green, and blue) and the stems were brown in the renderings. A large polygon coincident with the ground plane was specified as green. A blue sky filled the rest of the image.

Eye points used were various but the illumination point was usually maintained slightly above and to the side of the eye point.

The rendered images were used to verify the complex hierarchical descriptions for the 84 different 5, 7 and 9 compound leaves. In Fig. 5 we show a walnut tree reconstructed from detailed stem geometry measurements (Martens et al (1991)). A nadir view of an orchard with 25 walnut trees is shown in Fig.6. The description of the leaves is contained in a file of 400 kB size, the stem description is about 240 kB and the "prototype" leaf description is about 250 kB. Raytracing a tree with 37,175 elements for an image of 700 by 800 pixels takes about 10 minutes on a Sun SparcStation 10/41.

Some novel results can be derived from the walnut tree descriptions. From the *Rayshade* file we generated a data set containing the center of each compound leaf $\vec{P}_l$, the leaf area A_l and the mid rib orientation (Θ_l, Φ_l). First a volumetric data set was generated using the following steps :

1. Find the minimum and maximum extent of the leaf centers :

$$[x_{min},\ x_{max}];\ [y_{min},\ y_{max}];\ [z_{min},\ z_{max}]$$

2. Divide each range into a number $(N_x,\ N_y,\ N_z)$ of intervals. To avoid artificially large leaf area indices the product of two intervals (e.g. $\Delta x \Delta y$) should be less than the maximum compound leaf area :

$$\Delta_x\ =\ \frac{x_{max} - x_{min}}{N_x};\ \Delta_y\ =\ \frac{y_{max} - y_{min}}{N_y};\ \Delta_z\ =\ \frac{z_{max} - z_{min}}{N_z}.$$

3. For each leaf center $\vec{P}_l = [x_l,\ y_l,\ z_l]$ compute the volume element or voxel indices (i, j, k) :

$$i\ =\ INT[\frac{x_l - x_{min}}{\Delta_x}] + 1;\ j\ =\ INT[\frac{y_l - y_{min}}{\Delta_y}] + 1;\ k\ =\ INT[\frac{z_l - z_{min}}{\Delta_z}] + 1.$$

4. Increment the leaf density voxel: $A(i, j, k) = A(i, j, k) + A_l$.

5. The leaf area density LAD is then : $LAD(i, j, k) = A(i, j, k)/(\Delta_x \Delta_y \Delta_z)$.

6. By summing over all voxels in the z-direction a leaf area map can be produced as shown in Fig 7.

The leaf area index map produced showed some interesting features:

- The leaf area index is highly variable. While it averages near 5 there are some places where the LAI can be ten times larger.
- There are many empty spaces with no leaves where the ground is visible.

There are several consequences that arise are worth noting :

- The canopy spectral signature is a very complex average over many realizations with many different LAI's and contains spectral components of the background.
- It seems questionable that the LAI is a retrievable parameter because the canopy itself is highly variable and the retrieved number depends very much on the spacing of the trees. The non-unique relationship between LAI and canopy spectral indicators such as the Normalized Difference Vegetation Index or NDVI has been shown earlier by Jasinski (1990).

We also generated frequency plots for the zenith and azimuth angles of the mid rib orientation, which showed a plagiophil (peaked at 45^0) distribution in zenith angle and a uniform distribution for the azimuthal orientation. The mid rib zenith angle distribution was actually matched to field measurements (Martens, 1992).

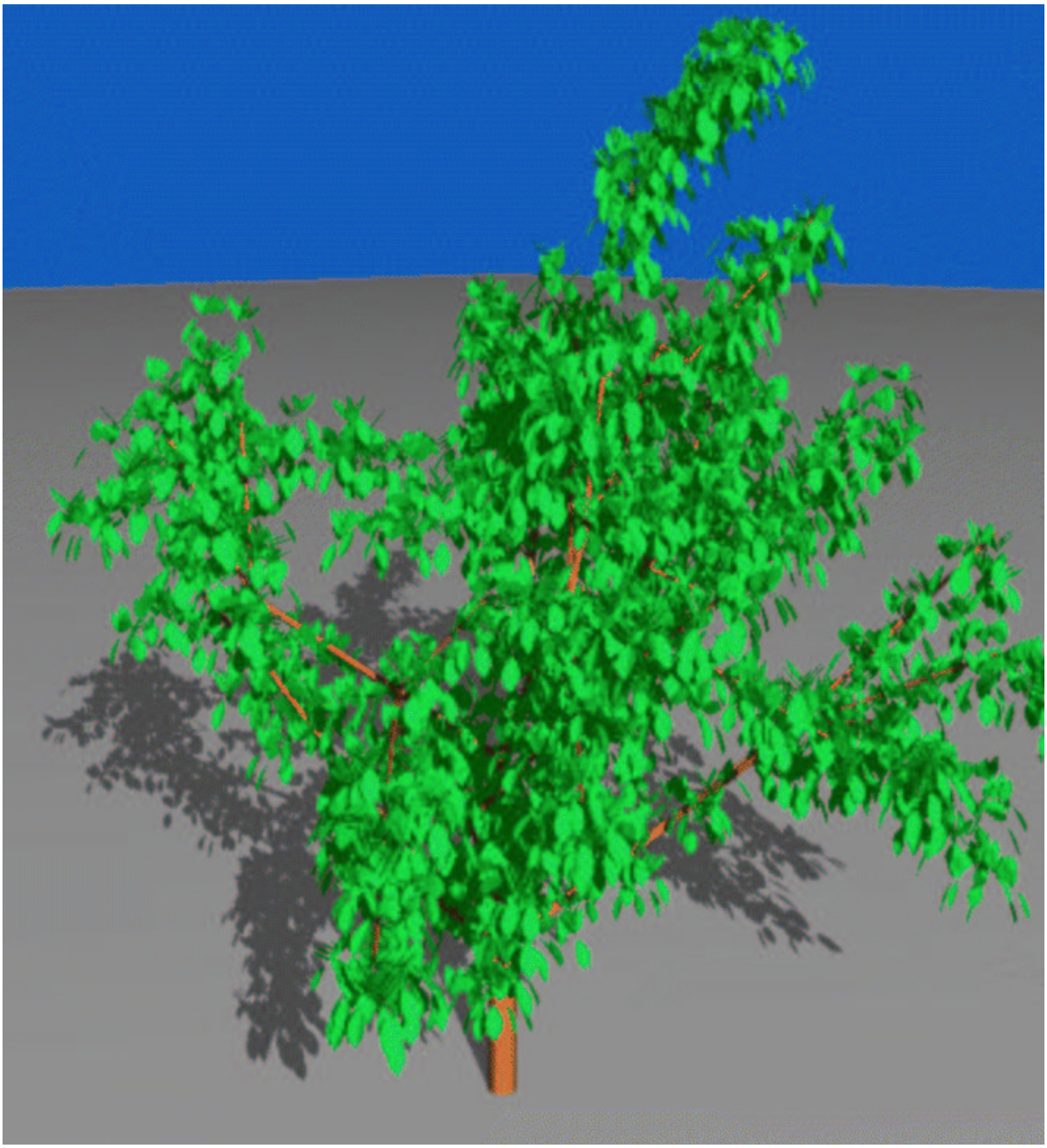

Figure 5: Reconstructed walnut tree rendered using raytracing

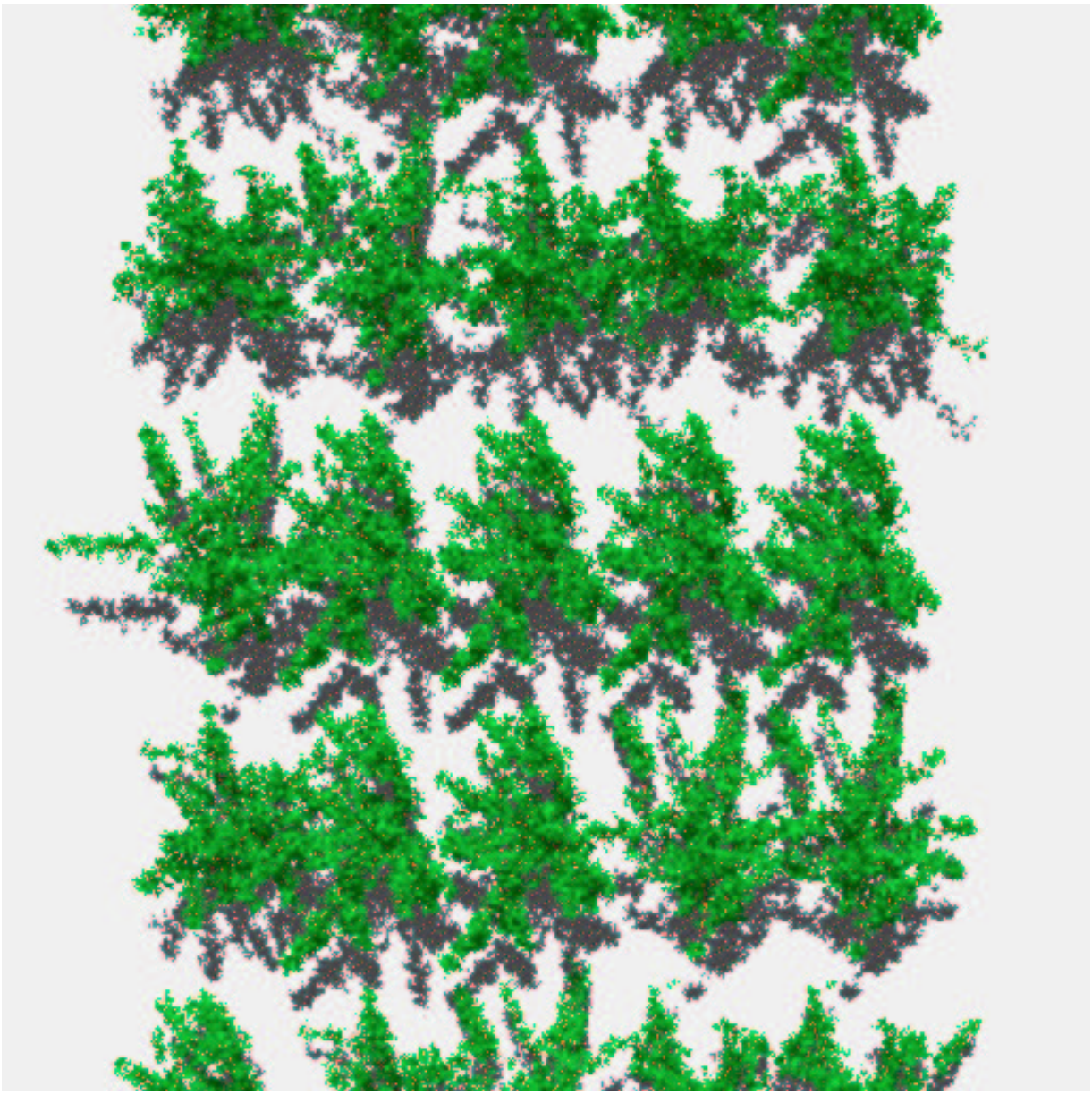

Figure 6: Walnut orchard rendered using raytracing

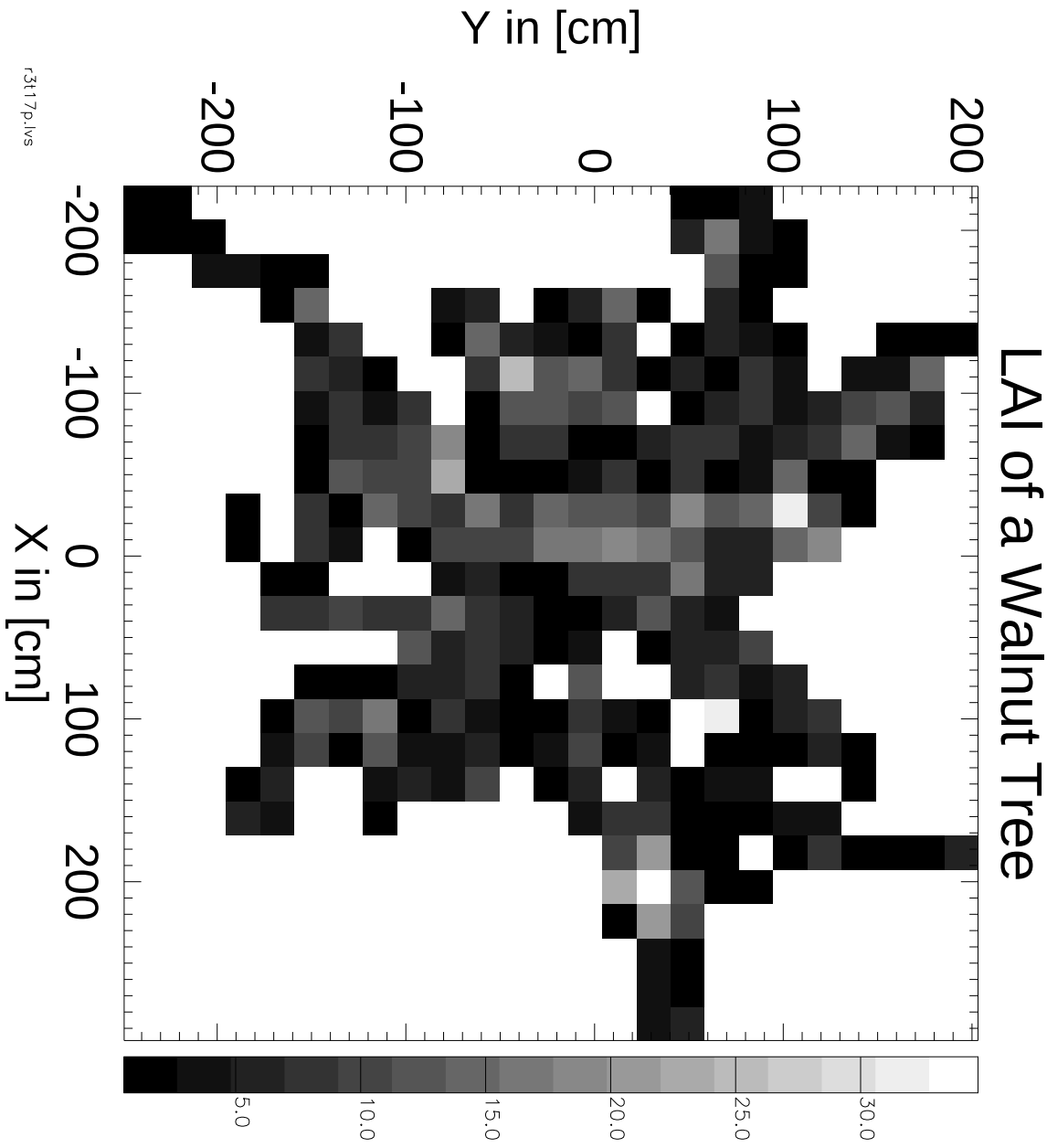

Figure 7: A leaf area index map for a walnut tree.

3.2 Douglas Fir Reconstruction

An experiment was performed at NASA Ames by Vanderbilt (Dungan et al, (1994))to study the effect of nitrogen fertilization on the canopy spectral signature. As part of the experiment Vanderbilt digitized the stem positions of six douglas fir seedlings in 3-D.

Our douglas fir reconstruction was done in several steps :

1. Display of 3-d data on PC using stick figures
2. Convert stem data to a linked list (same as walnut data)
3. Compute needle orientation (using DF samples from Los Alamos) assuming that :
   (a) the divergence angles are normally distributed with mean of 60^0 and standard deviation of 10^0
   (b) and the phyllotaxy angles are normally distributed with mean of 60^0 and standard deviation of 10^0
4. Needle densities vary with up to 40 needles per cm
5. Needle positions uniformly spaced along segment
6. Needle lengths from 1.2 cm to 2.7 cm
7. Needle shape is a rectangular box with cross section 1.5 mm by 0.5 mm
8. Generate *Rayshade* files for each tree and
9. render on cluster of 16 IBM RS6000 workstation (CPU time from 20 min to 1.2 h for images 512 x 640)

An example of a reconstructed tree is shown in Fig. 8.

We produced LAI maps for the douglas fir seedlings using the same approach as for the walnut trees. The LAI varied again from very small values to larger values. The concept of describing a canopy using LAI seemed again not very useful because of the small cross section of the needles. In Figure 9 we show another visualization of the 3D structure of one of the douglas fir seedlings. The position of the center of each needle is indicated by a cross. The horizontal axis is the x direction and the vertical axis is the z direction. The color of the cross indicates the distance of a needle in the y direction according to the color bar on the right side of the plot in cm. In Figures 10 and 11 we show histograms of the needle orientation in zenith and azimuth. Note that the needles seem to prefer an almost horizontal orientation similar to a planophil distribution. The azimuthal distribution is close to uniform. In Figure 12 we show the needle reflectance and canopy BRF for each fertilization level. Note that the needle and canopy spectra are very similar for low and medium fertilization levels but differ for high fertilization levels.

3.3 Maple Seedling Reconstruction

In a study conducted by Barbara Yoder at Oregon State University in Corvallis, OR, big leaf maple seedlings were treated with three different amounts of fertilization to establish a wide variation in concentration of chlorophyll and nitrogen (Yoder and Pettigrew (1994)). The goal was to examine the interactive effects of two biological factors, leaf density and chemical concentration, on spectral features in an experimental setting in which other influencing factors could be held reasonably constant (Yoder (1993)).

Detailed measurements were made of the architecture of 21 individual trees (7 from each fertilization treatment). For each stem the stem base (node) was digitized in three dimensions and the point where a leaf is attached (petiole). For each leaf the leaf angle, the leaf width and length were measured. From digitized leaf silhouettes we generated a polygon for a maple leaf which was then scaled according to the measured

Figure 8: Reconstructed douglas fir tree

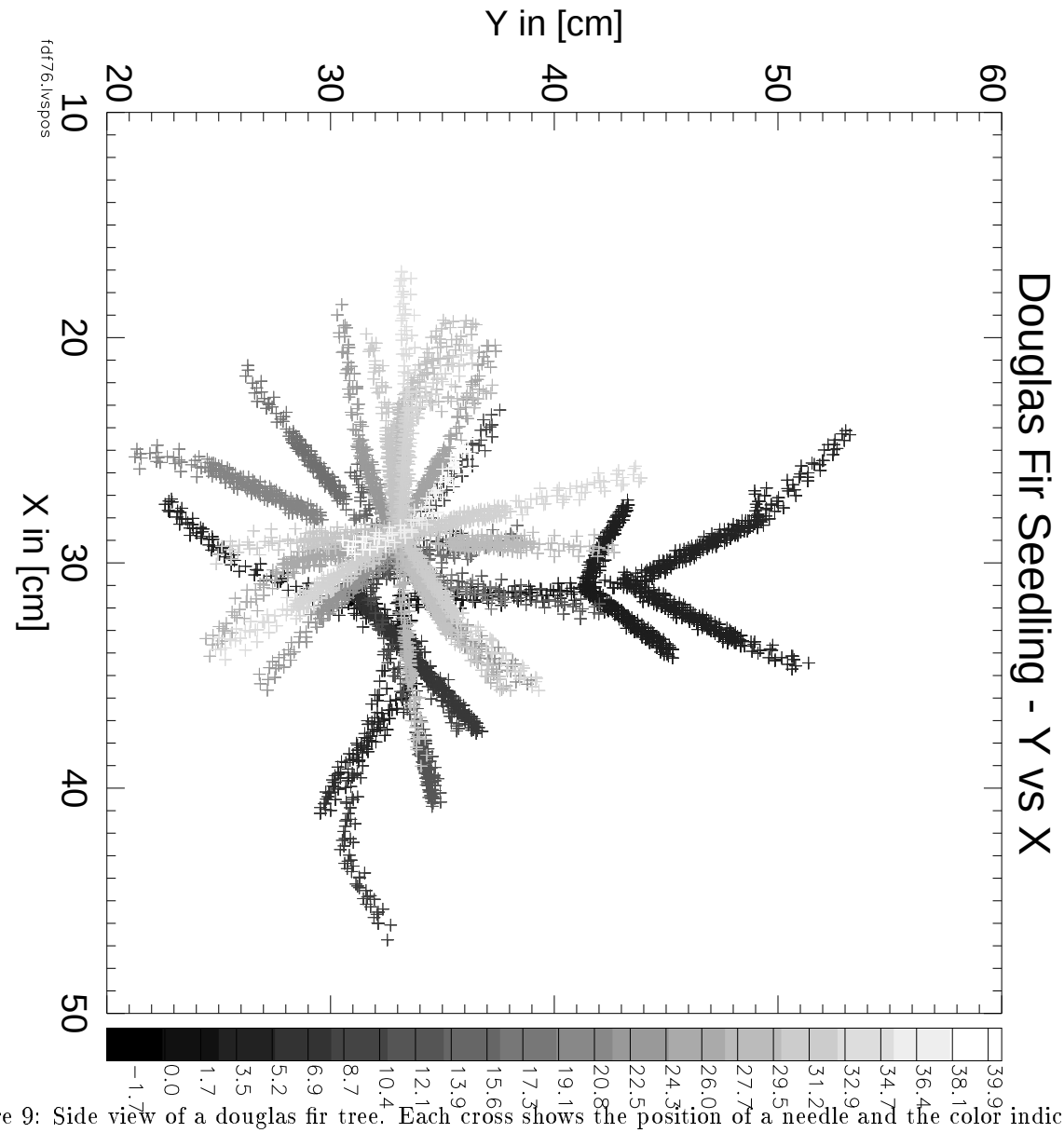

Figure 9: Side view of a douglas fir tree. Each cross shows the position of a needle and the color indicates the y position in cm.

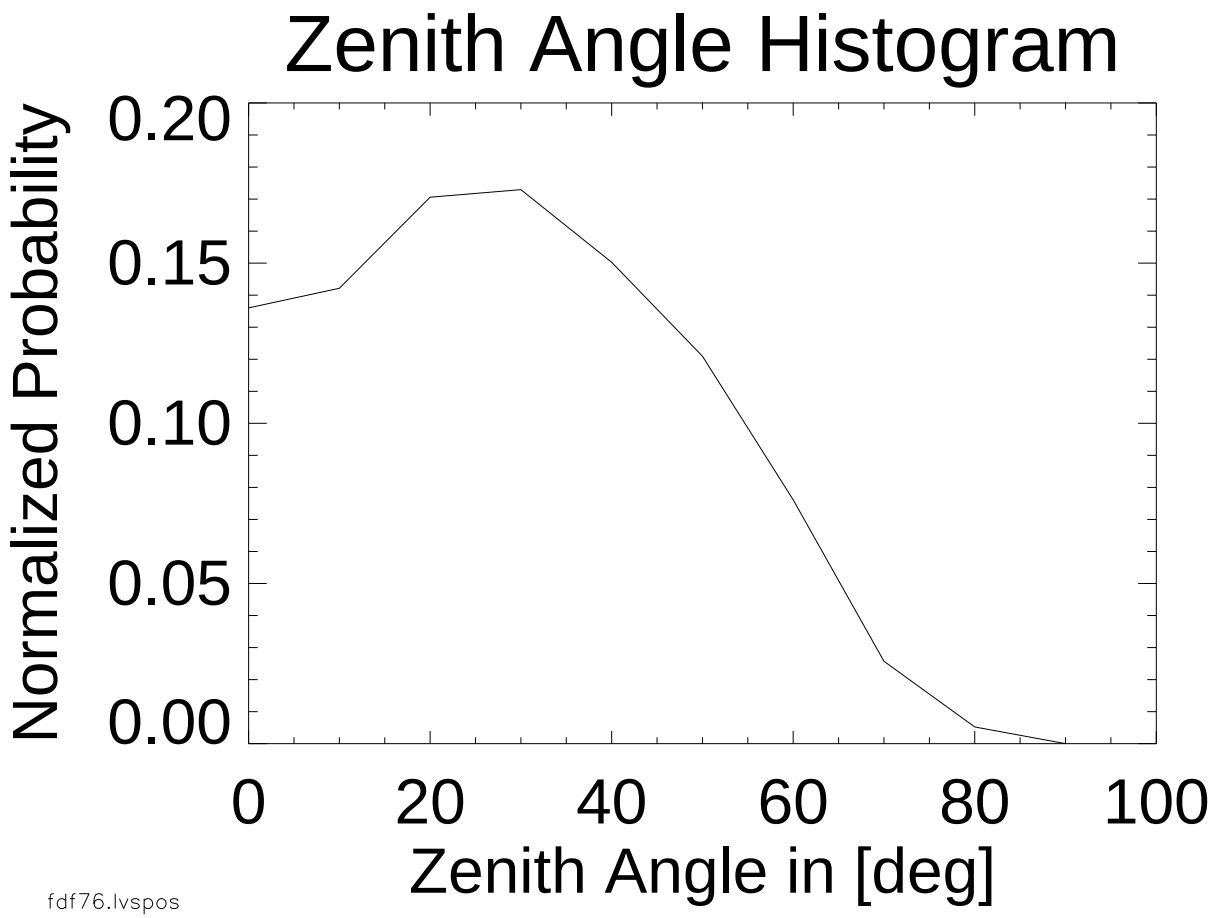

Figure 10: Histogram of the needle zenith angle of a douglas fir seedling

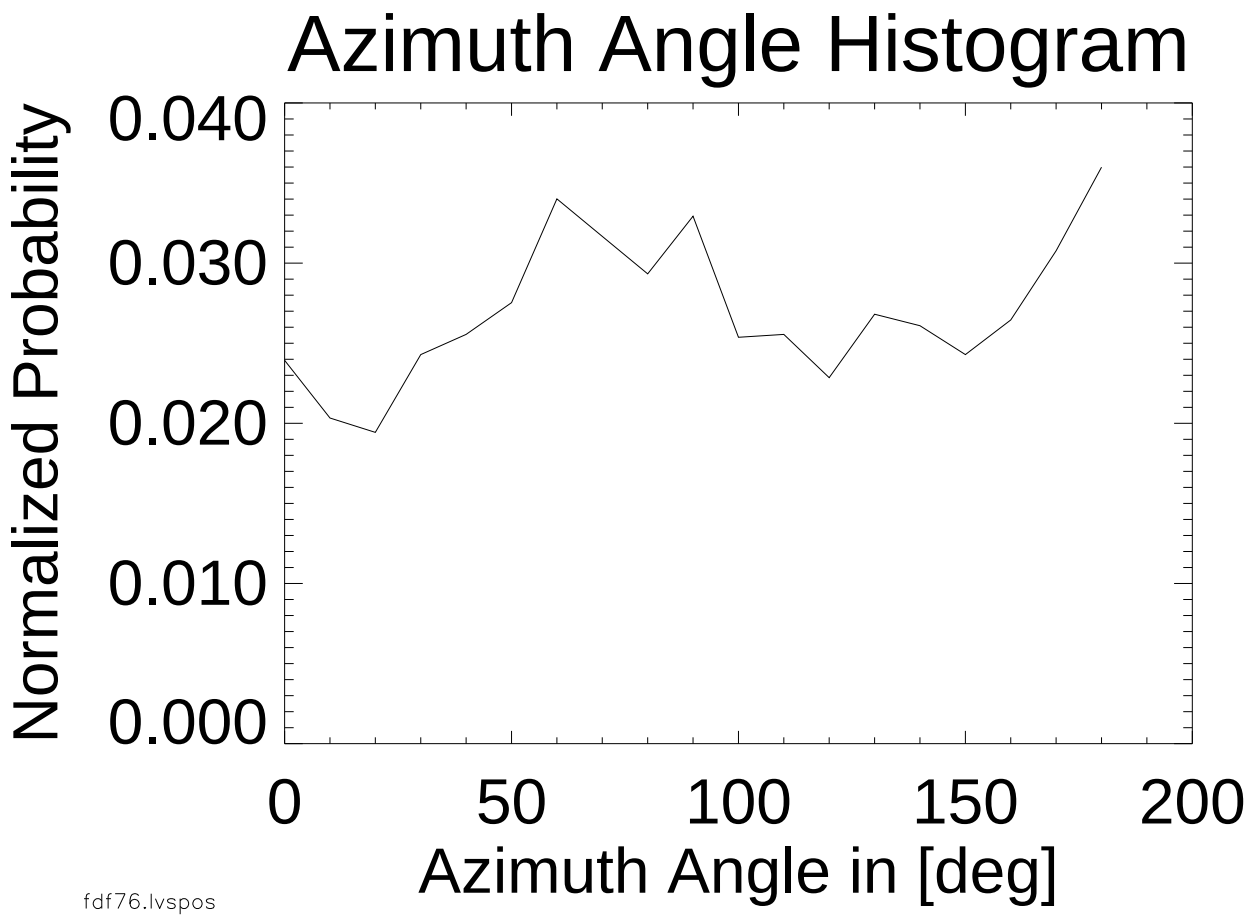

Figure 11: Histogram of the needle azimuth angle of a douglas fir seedling

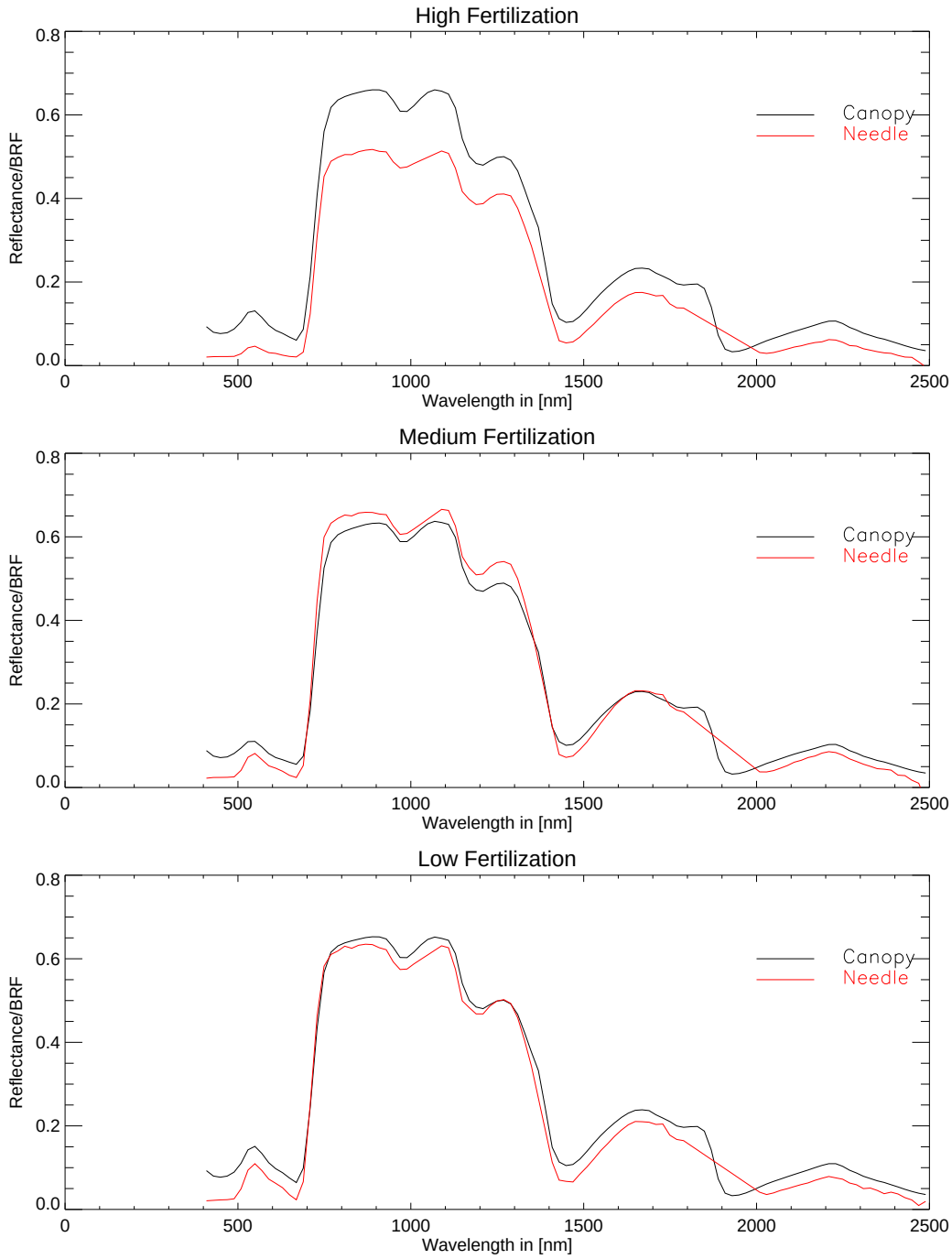

Figure 12: Needle reflectance and canopy BRF for low, medium and high fertilization level

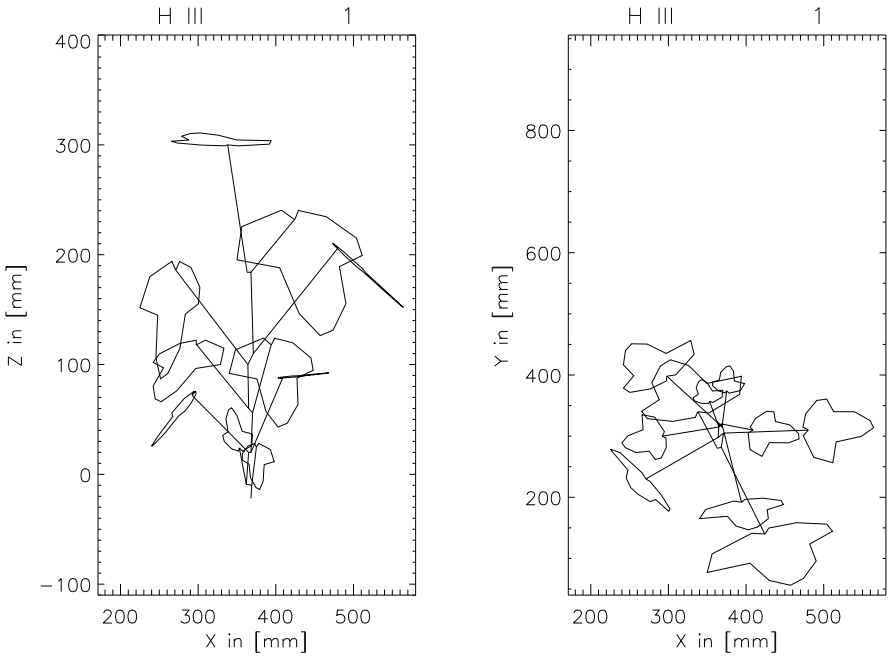

Figure 13: Reconstructed line drawing of a big leaf maple seedling

leaf dimensions and attached to the stems using the direction from the main stem to the petiole position as the azimuth angle, which was not measured originally. Thus we produced 21 different trees that could be arranged to simulate the miniature canopies. Line drawings such as the one shown in Figure 13 were used to visualize all trees before they were combined to canopies.

Fig. 14 shows an image of an individual big leaf maple seedling.

Putting randomly selected seedlings into three different canopy densities we produced nine different canopies. The effect of azimuthal illumination direction is shown in Fig. 15. Leaf level measurements of the reflectance and transmittance of big leaf maple leaves from the top side (adaxial) and bottom side (abaxial) showed some differences in the spectra. The green peak decreased with increasing fertilization. Three spectra are shown in Figure 16.

Measured canopy spectra were noisy because the windy conditions caused the leaves to move while the spectrometer scanned through the wavelengths from $0.4\mu m$ to $2.5\mu m$ at the time of the outdoor measurements. Figure 17 shows the canopy level spectra for the three fertilization treatments, where H is the high, M is the medium and L is the low level treatment. The type of canopy measured is indicated with the last letter of the label: F is a full canopy, H is a half canopy and Q is a quarter canopy. As one would expect the dense canopies produced the highest reflectance levels.

4 Reflectance Spectra for Simple Canopies

4.1 Stacked Leaf Experiment and Model Calculation

To illustrate the basic nonlinear effects due to the canopy structure, we will compute the reflectance of a stack of leaves. Experimental results have been described by Swain and Davis (1978). Later Cooper, Smith and Pitts (1982) developed a canopy model based on the adding method which can be used to derive the overall reflectance of a stack of leaves. In a previous paper (Borel and Gerstl (1994)) we described nonlinear

Figure 14: Reconstructed big leaf maple seedling

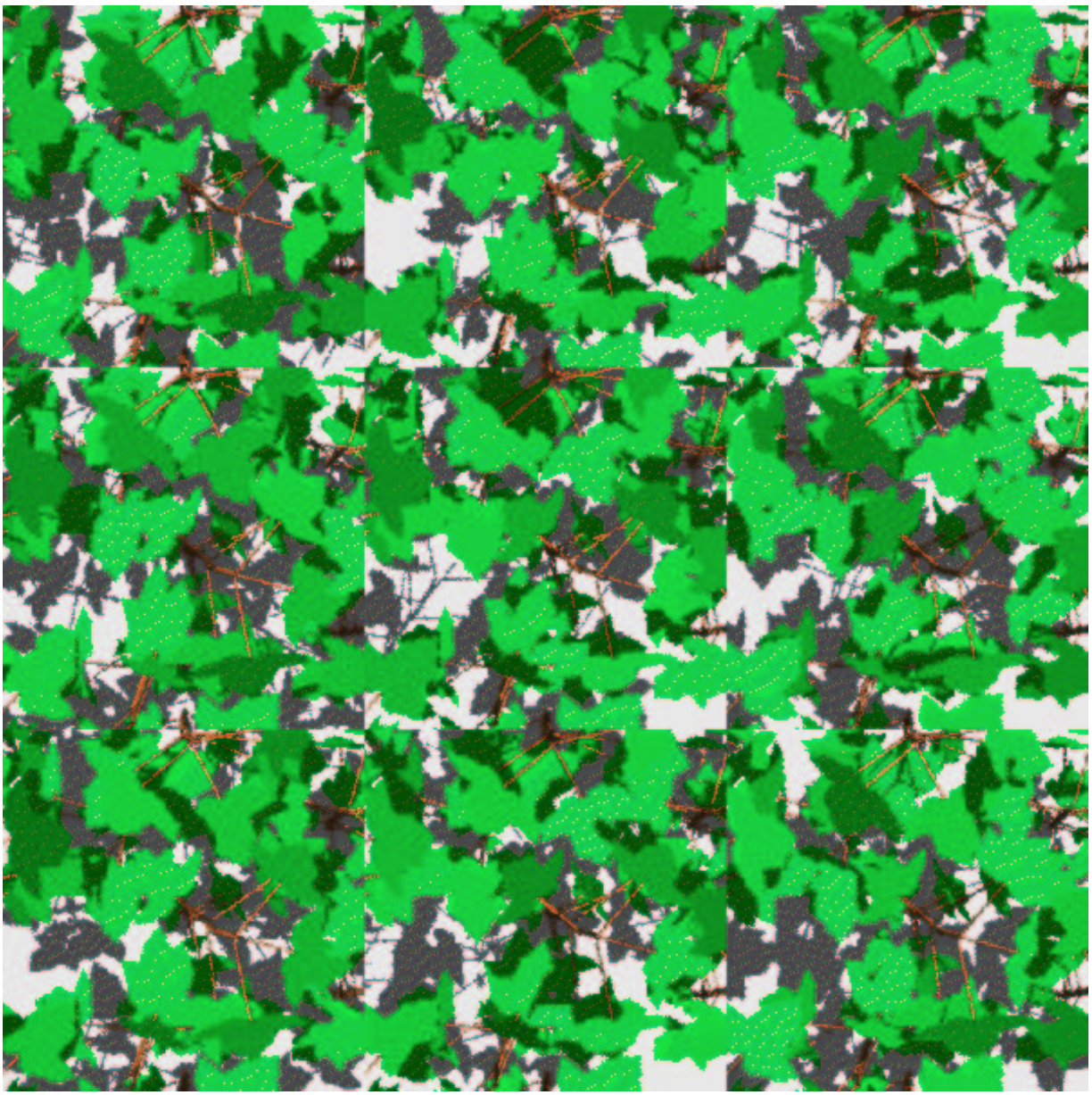

Figure 15: Reconstructed big leaf maple seedling canopy for the medium fertilization level and a half filled canopy for 9 different sun azimuth angles and a sun zenith angle of 25 deg for a nadir viewing direction.

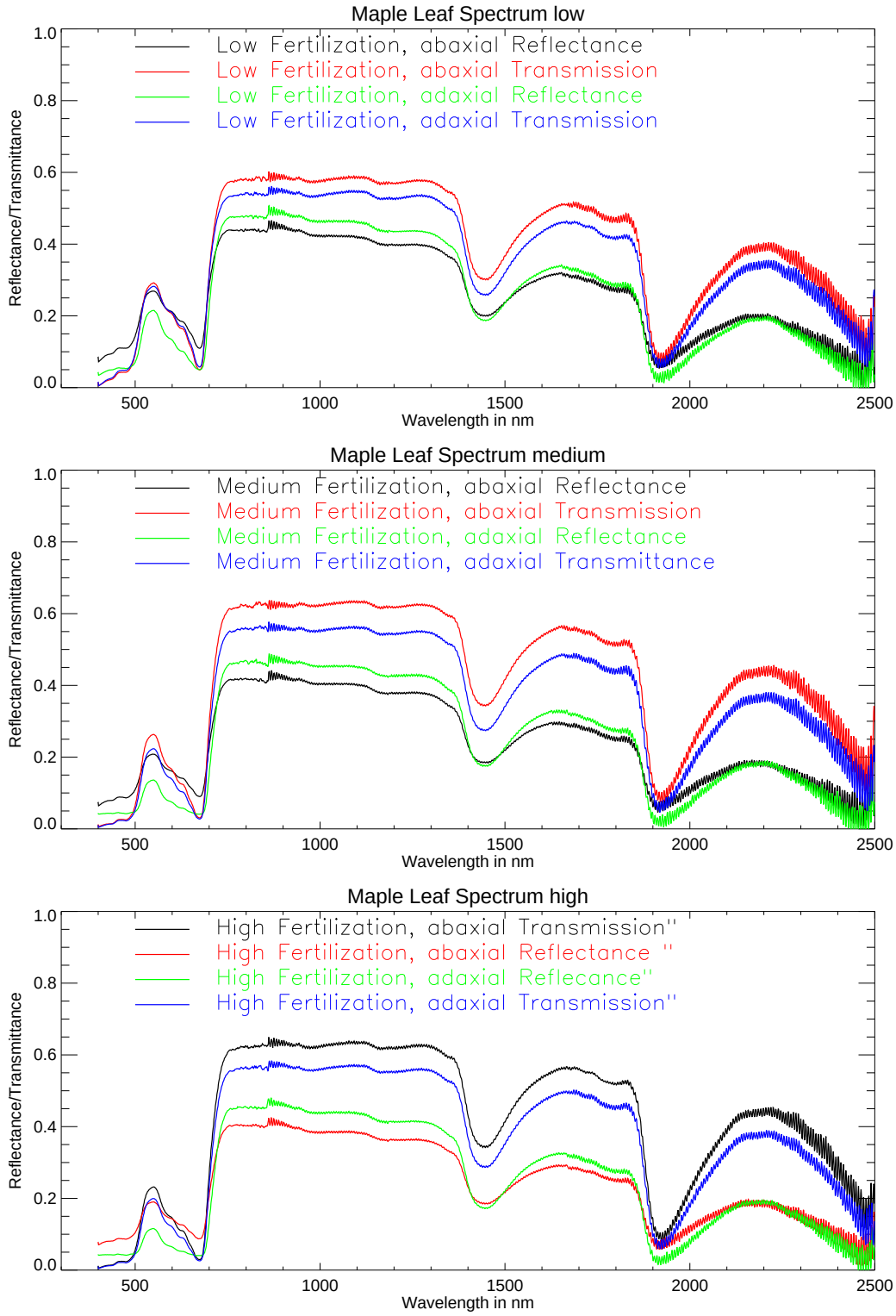

Figure 16: Measured Reflectance/Transmittance of big leaf maple leaves treated with three different levels of fertilization

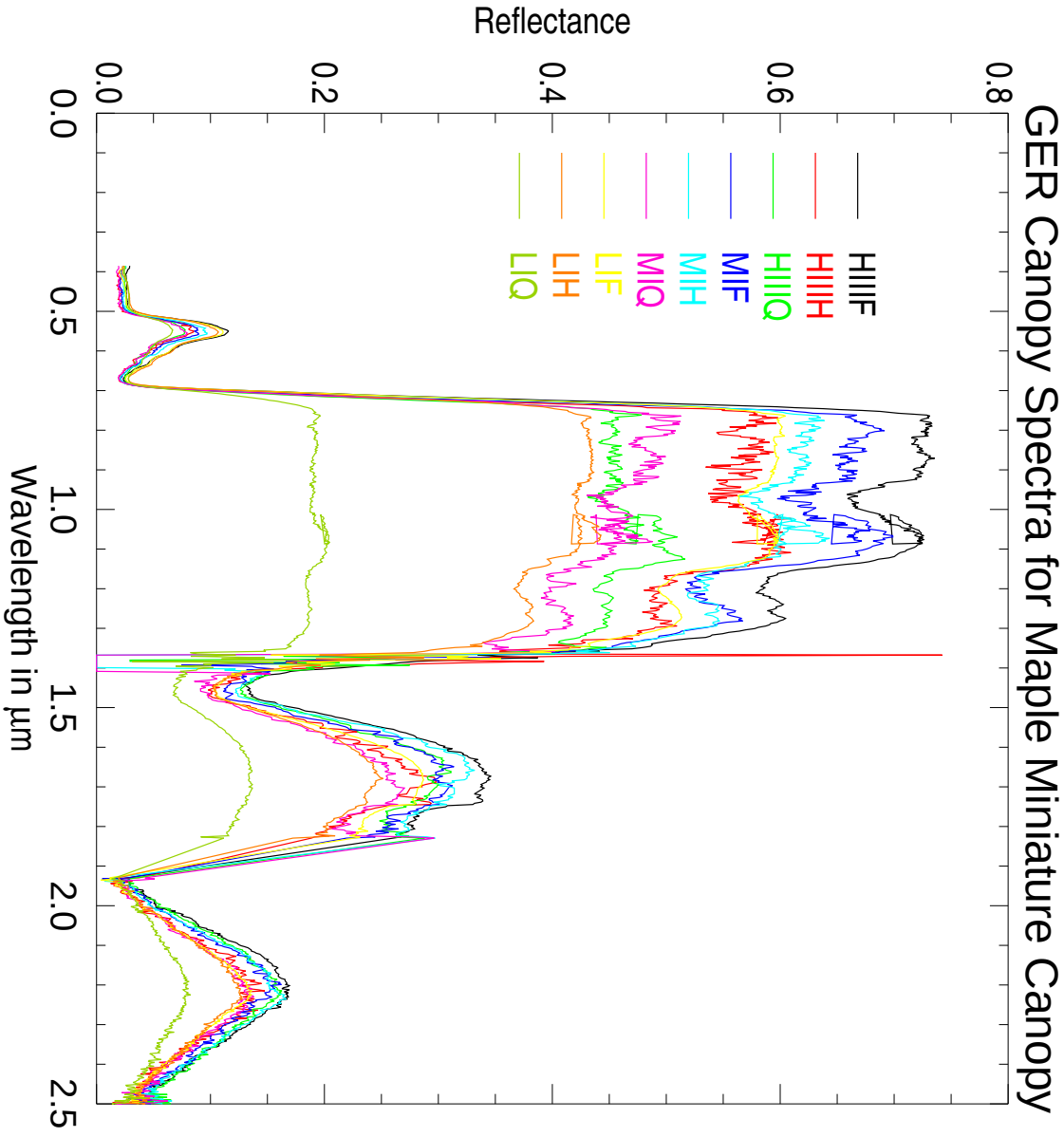

Figure 17: Measured canopy spectrum of three fertilization treatments (L, M, H) and three canopy densities (F, H, Q)

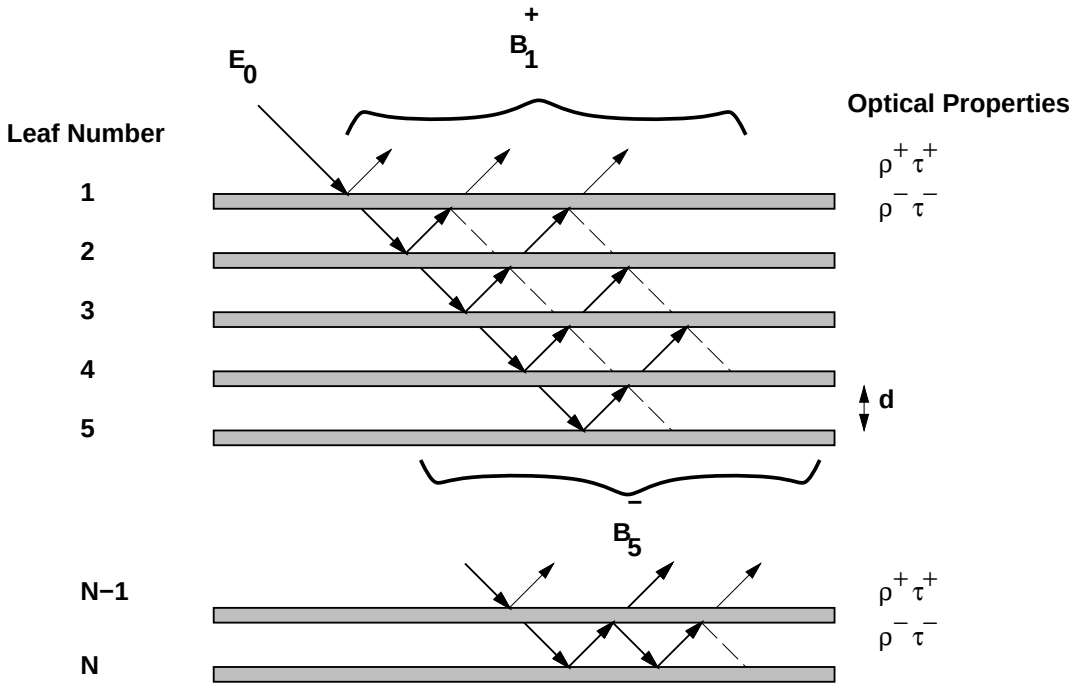

Figure 18: Geometry of a stack of leaves

spectral mixing models for vegetative and soil surfaces.

In Fig. 18 we show the geometrical arrangement under consideration. The leaves are assumed to have side dependent (upper and lower side) reflectance and transmittance values as a function of wavelength. The upper side has the subscript + and the lower side −. First we assume that the spacing is as small as possible to allow for an air gap between leaves. Using the multi-layer concept as described by Borel, Gerstl and Powers (1991), all light incident on the top surface of the second, third,.. N-th leaf is the sum of the reflected light from the lower side of the layer above and transmitted light from the layer below. For the n-th leaf, where $n \neq 1$ or $n \neq N$ we can express the radiosity B_n^+ as :

$$B_n^+ = \rho^+ B_{n-1}^- + \tau^- B_{n+1}^+, \quad n = 2, 3, 4, \ldots, N-1. \tag{1}$$

Similarly for the radiosity on the underside (B_n^-) we get :

$$B_n^- = \rho_- B_{n+1}^+ + \tau^+ B_{n-1}^-, \quad n = 2, 3, 4, \ldots, N-1. \tag{2}$$

The radiosity for the top leaf surface is the sum of the reflected incident light E_0 and the transmitted light from the second layer or :

$$B_1^+ = \rho^+ E_0 + \tau^+ B_2^+ \tag{3}$$

and similarly the radiosity on the bottom side is the sum of the transmitted incident light and the reflected light from the top of the second layer or :

$$B_1^- = \tau^+ E_0 + \rho^- B_2^+. \tag{4}$$

The radiosities (up and down) on the N-th layer can be derived from eqs (1) and (2) by excluding out the terms for the $(n+1)$-th layer :

$$B_N^+ = \rho^+ B_{N-1}^- \tag{5}$$

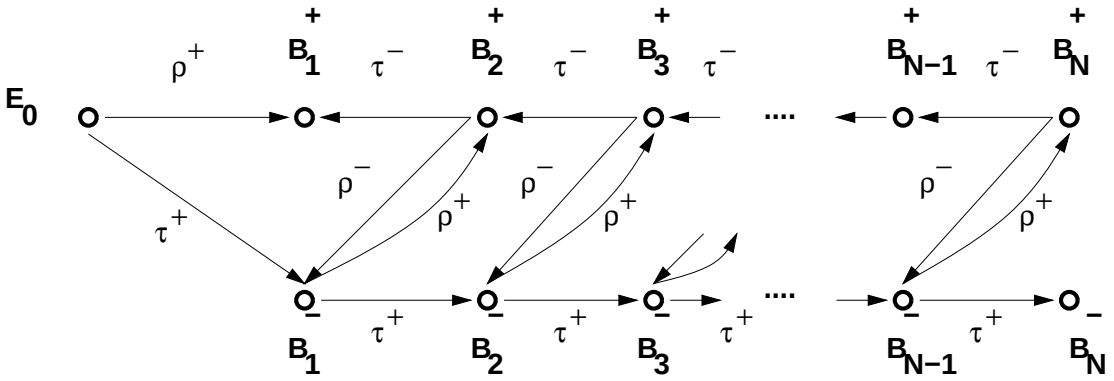

Figure 19: Network representation of the multiple reflections inside a stack of leaves

and

$$B_N^- = \tau^+ B_{N-1}^-. \tag{6}$$

This system of equations can be solved analytically for a given number of layers (see Borel, Gerstl and Powers (1991)) but we will not do this here. Rather we want to show another way of displaying the system of equations as a network of nodes (radiosities) and directed paths (reflectances and transmittances). The network is shown in Fig. 19. It is easy to obtain the radiosity equation for a node by adding all incoming arrows' values multiplied with their source values. It is also possible to compute the overall reflectance ρ_{total} by dividing the radiosity of the top surface of layer 1 (B_1^+) through the incident energy flux per unit area (E_0) or :

$$\rho_{total} = \frac{B_1^+}{E_0}. \tag{7}$$

In terms of network theory (see Moschytz (1974)), this ratio is a transfer function and can be obtained using Mason's rule. Note that the above equations can be derived from the N-layer canopy model described in Borel, Gerstl and Powers (1991, p.26) by setting lai to 1.

We will now show some experimental results obtained by measuring the up/down reflectance and transmittances of leaves and various stacking configurations in the visible using an external calibration sphere and a spectrometer. The radiosity equations (1 - 6) were solved iteratively starting with $B_n^{+/-} = 0, n = 1, \ldots, N$ and $E_0 = 1$. Fig. 20 shows the measured conical/hemispherical reflectances and transmittances of a single leaf.

Fig 21 shows the measured and computed reflectances above the leaf stack as a function of the number of stacked leaves.

The agreement between the computed and measured data for stacks with $N = 2, 3, 4, 5$ is very good except near 730 nm. We found that aspen leaves have a chlorophyll emission maximum near 735 nm according to Lichtenthaler (1989), which may be responsible for the overestimated ρ of the stack. The reason for a higher total ρ is that the measured leaf reflectances and transmittances are too high due to fluorescence near 735 nm causing the multiple reflections/transmissions to be higher.

This derivation using the radiosity method is not new or different from other methods such as the adding or doubling method. If, however, spacing between the finite leaves and partial illumination of a leaf is included, the adding method cannot be used anymore because it does not include view factors or allow partial illumination.

If all leaves have the same orientation, spacing d and are aligned, one finds that a leaf in the stack does not receive all reflected or transmitted light from the adjacent leaf. Some of the light will leak out of the stack and will be lost. The fraction of light trapped which will interact again with a surface is given by the

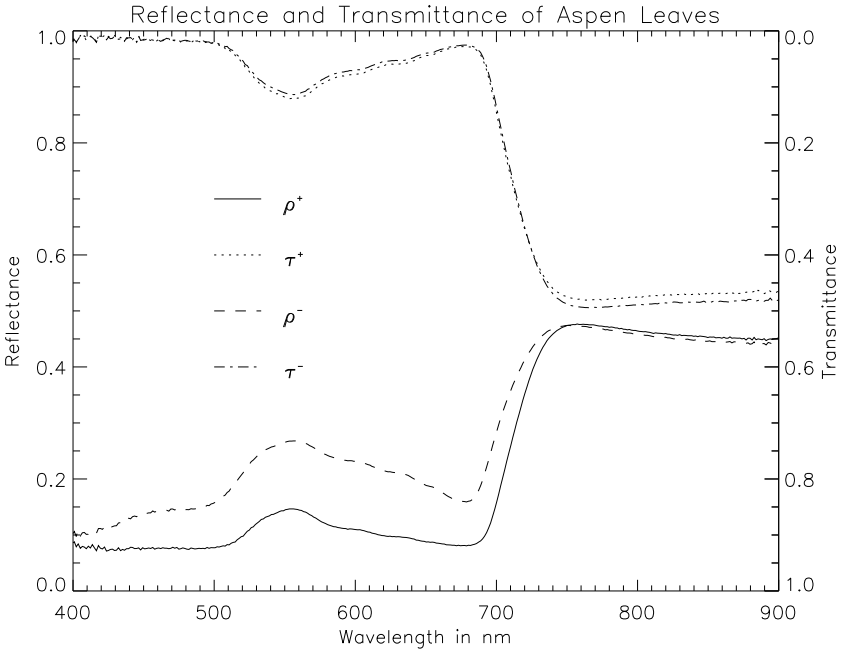

Figure 20: Measured reflectances and transmittances for an aspen leaf

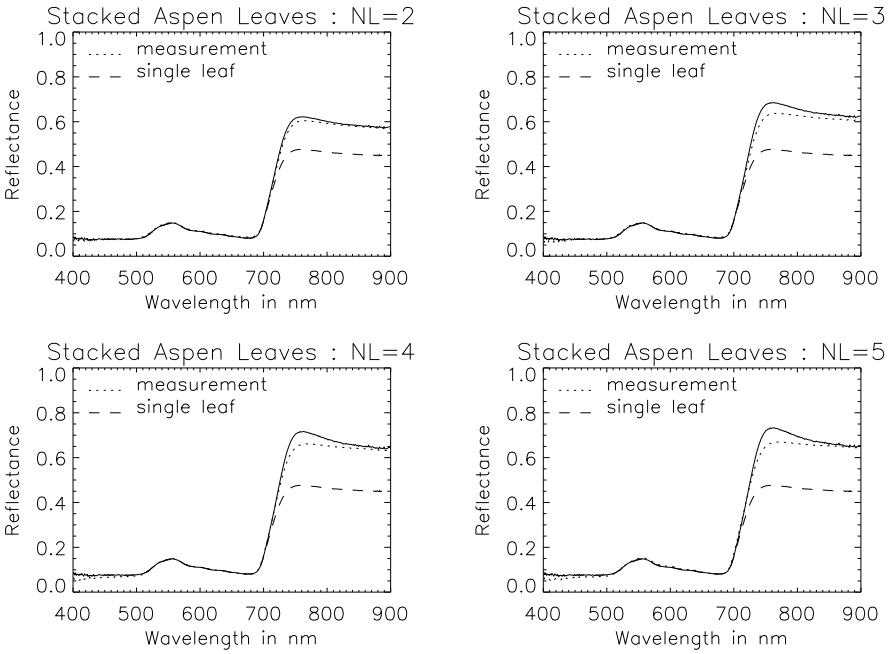

Figure 21: Comparison of measured and computed total reflectances for stacks of 2,3,4 and 5 aspen leaves

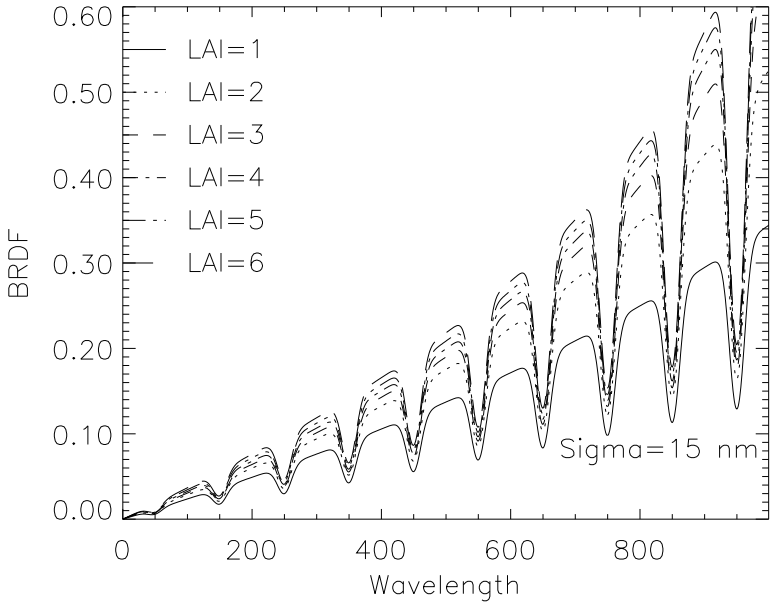

Figure 22: N-layer radiosity model demonstrates nonlinear effects on an absorption feature

view factor F_{ij} (see Borel, Gerstl and Powers (1991)). Tables exist for analytic view factors between plates of different shapes, such as disks and squares in various geometric relationships, e.g. Hottel and Sarofim (1967). Simple numerical methods exist to compute view factors between polygons, e.g. Baum, Rushmeier and Winget (1989). Partial illumination of a leaf inside the stack can be taken into account by adding the surface averaged incident energy per unit area E_0 over the leaf surface. In the network representation this corresponds to adding arrows from E_0 to all the B_n^+ and B_n^-, $n = 1, 2, 3, \ldots, N$ with weights according to their fraction of illumination. It is possible to add the effects of ground surfaces and indirect illumination from the sky by simple extensions.

4.2 Absorption Model using the N-Layer Model

A simple model using artificial absorption features was developed to show the effect of nonlinear spectral mixing :

- Let $\rho = \tau$ be a linear function of wavelength from 0. to 0.5 and add 10 absorption features with a mean and standard deviation (Sigma)
- Compute BRDF of a layered canopy with $N = 10$ layers for leaf are indices per layer of LAI from .1 to .6

In Fig.22 we show how the absorption features change as a function of LAI. The modulation depth was always set to 50 % of the level of the reflectance/transmittance near the absorption. Note that the higher the LAI gets the more the originally linear BRDF envelope of the maxima appears nonlinear . The location of the minima does not change significantly because light is absorbed in the leaves. From this model we concluded that absorption features in leaves are preserved at the canopy level and may even be enhanced. The relationship between the concentration of a leaf chemical constituent and its spectral signature is nonlinear

at the canopy level. Thus for quantitative canopy chemistry retrievals it is necessary to model the influence of the canopy architecture.

5 Canopy Spectral Signature of Complex 3D Canopies

Because of its desired simplicity we developed a hybrid model to calculate the canopy spectral signature of an orchard of walnut trees. We are not able to deal with large numbers of surfaces in our radiosity model yet, because an orchard of 25 walnut trees contains about 10^6 polygons, cylinders and spheres. Such a large number of objects would require over 10^{12} matrix elements for the radiosity equation. To compute the viewfactors, assuming only 1000 rays per object would require over 10^9 rays. The *true* radiosity method would require vast computing and storage requirements.

The leaf reflectance and transmittance and soil reflectance is shown in Figure 23. The hybrid model has the following steps :

1. Raytrace images of a part (2 m x 2 m) of a reconstructed walnut tree for a given geographical location (e.g. Maricopa or Los Alamos or 45^0 North latitudes) and dates (e.g. March-21, May-26, June-21) and given times (e.g. every hour from 8 am to 4 pm) for nadir view or off-nadir views ($\theta_v = -40^0, -30^0, .., +30^0, 40^0$).

2. Compute image statistics such as (see Borel and Gerstl (1994)):

- Probabilities of seeing illuminated surfaces :

  $P_{leaf}^{sun},\ P_{bark}^{sun},\ P_{soil}^{sun}$

- Probabilities of seeing shaded surfaces :

  $P_{leaf}^{shade},\ P_{bark}^{shade},\ P_{soil}^{shade}$

  An example of how the probability of seeing illuminated and shaded surfaces changes as a function of view directions and of sun directions is shown in Figures 24 and 25. Note that the probability of seeing shaded leaves is usually greater than that of seeing illuminated leaves. Thus it is important to be able to compute good shade spectra which is possible using the radiosity method.

- Average cosine of angle between the surface normal and sun vector for visible illuminated surfaces :

  $\overline{(\vec{n}_{leaf} \cdot \vec{n}_{sun})},\ \overline{(\vec{n}_{bark} \cdot \vec{n}_{sun})},\ \overline{(\vec{n}_{soil} \cdot \vec{n}_{sun})} = \cos\theta_s$

An example of how the average cosine between the surface normal and sun vector for visible illuminated surfaces changes as a function of view directions and of sun directions is shown in Figures 26 and 27. Since the brightness of Lambertian surfaces varies with the cosine of the incidence angle we can call the average cosine also normalized intensity. Note that the average soil intensity was normalized to unity in Figure 26.

3. Approximate radiosities for the canopy by using the N-layer model (see Borel and Gerstl (1994, p.409)) with a total LAI similar to the walnut canopy ($LAI = 5$), measured leaf reflectances ρ and transmittances τ and assumed soil reflectance ρ_s ($\rho_{bark} = 0.$) :

$$\overline{B_{leaf}^{sun}} = \sum_{n=1}^{N} B_{leaf,n}^{sun} lai(1-lai)^{n-1},$$

$$\overline{B_{leaf}^{shade}} = \sum_{n=2}^{N} B_{leaf,n}^{shade} lai(1-lai)^{n-1},$$

B_{soil}^{sun} and B_{soil}^{shade}. An example of the spectra on illuminated leaves and soil is shown in Figure 28. The labeling of the curves represent the spectra for different LAI's of a canopy. The soil spectrum was generated using SOILSPEC. Note the increasing radiosity on the leaves with increasing LAI and the decreasing radiosity at the ground.

4. Approximate the spectral BRDF $f_{canopy}(\cdot)$ of the walnut canopy by :

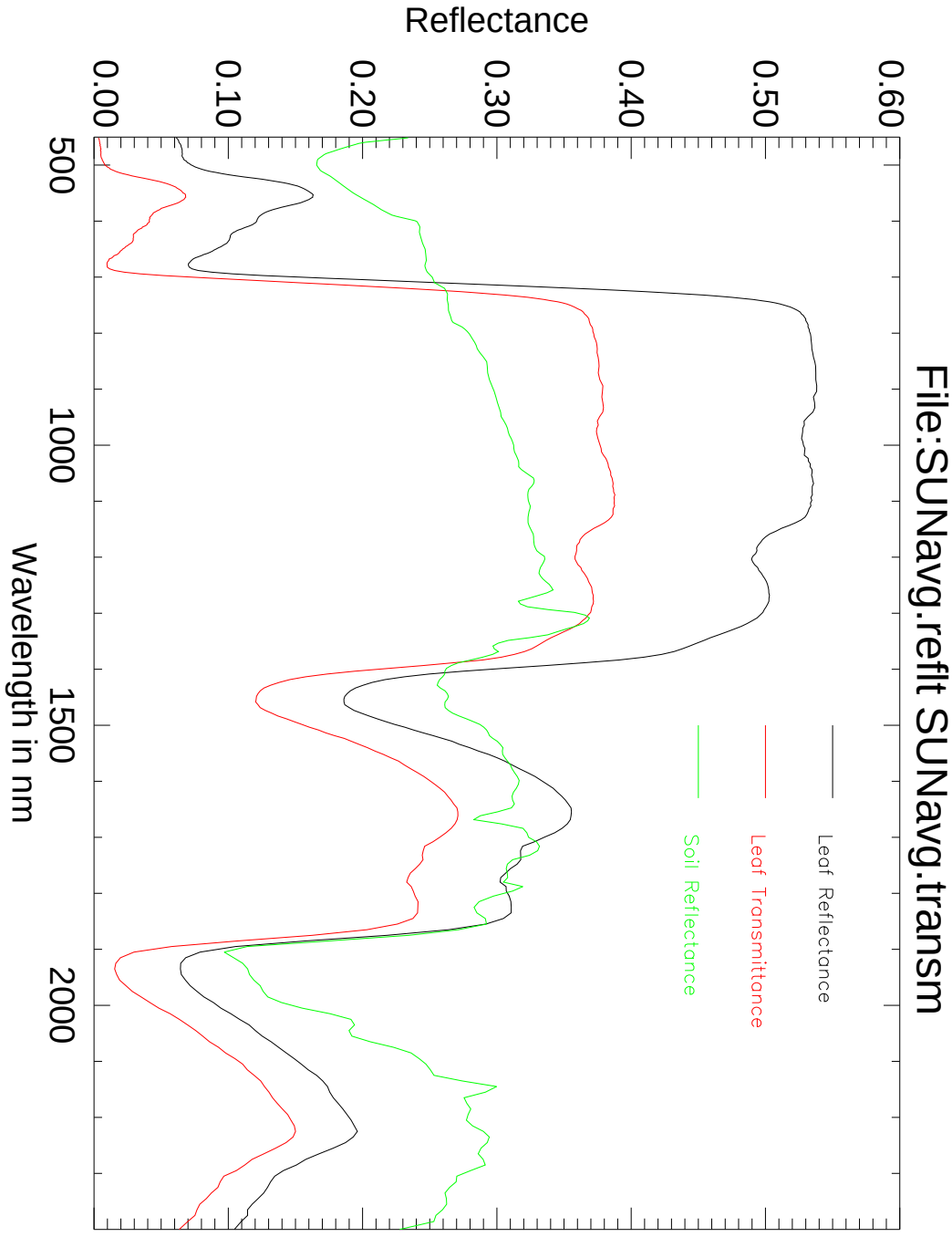

Figure 23: Leaf reflectance and transmittance of walnut leaves and a soil spectrum

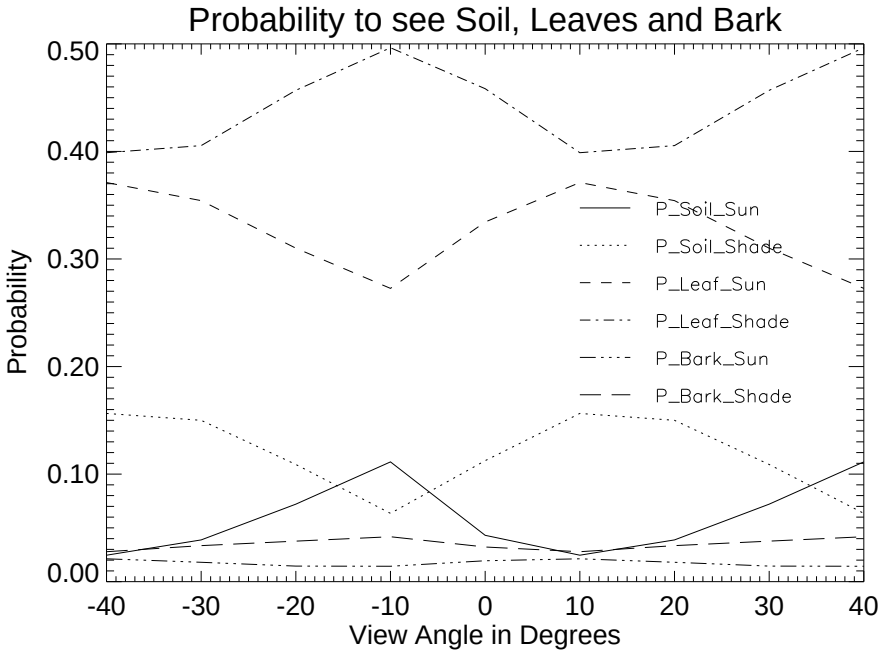

Figure 24: Canopy averaged probabilities of seeing illuminated and shaded surfaces for a walnut tree from different view directions

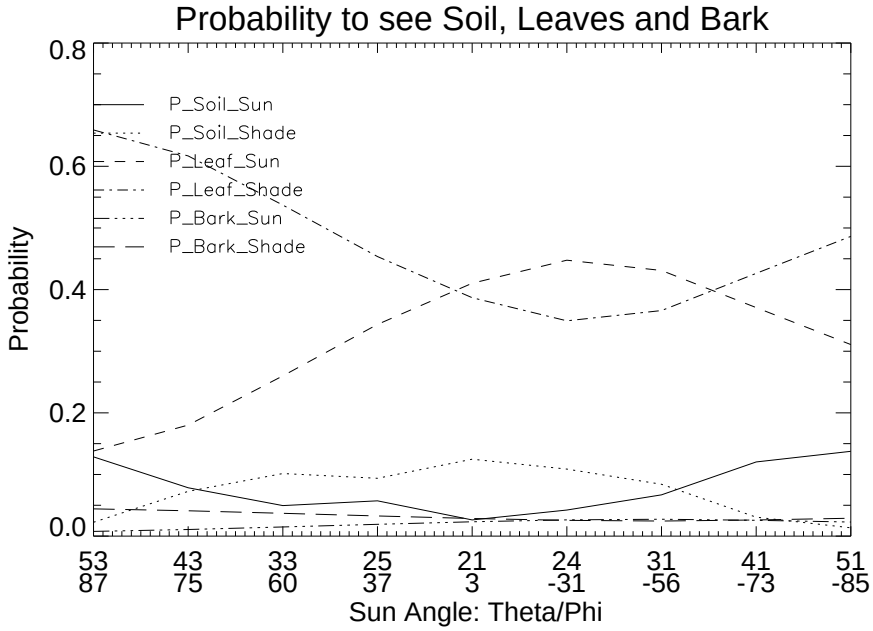

Figure 25: Canopy averaged probabilities of seeing illuminated and shaded surfaces for a walnut tree from nadir view

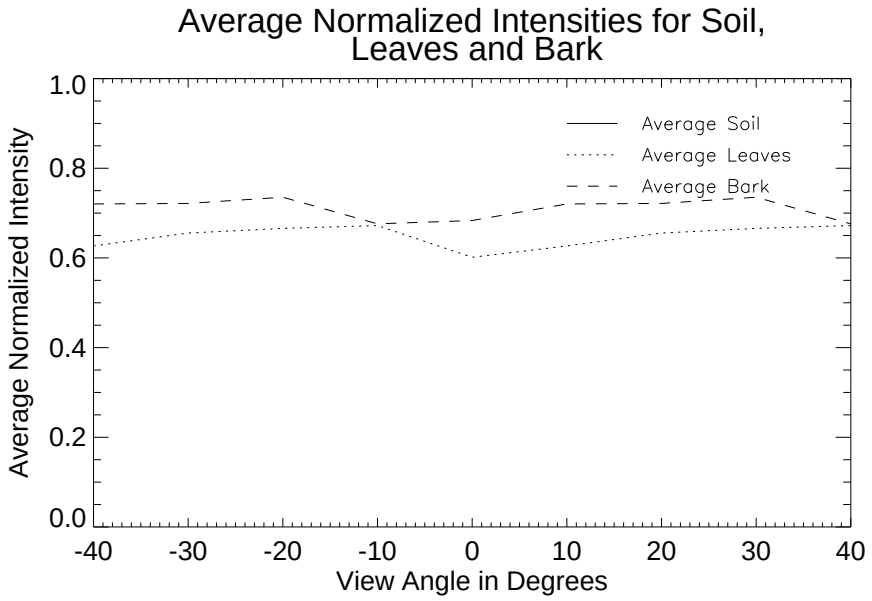

Figure 26: Average cosine of angle between the surface normal and sun vector for visible illuminated surfaces as a function of view directions

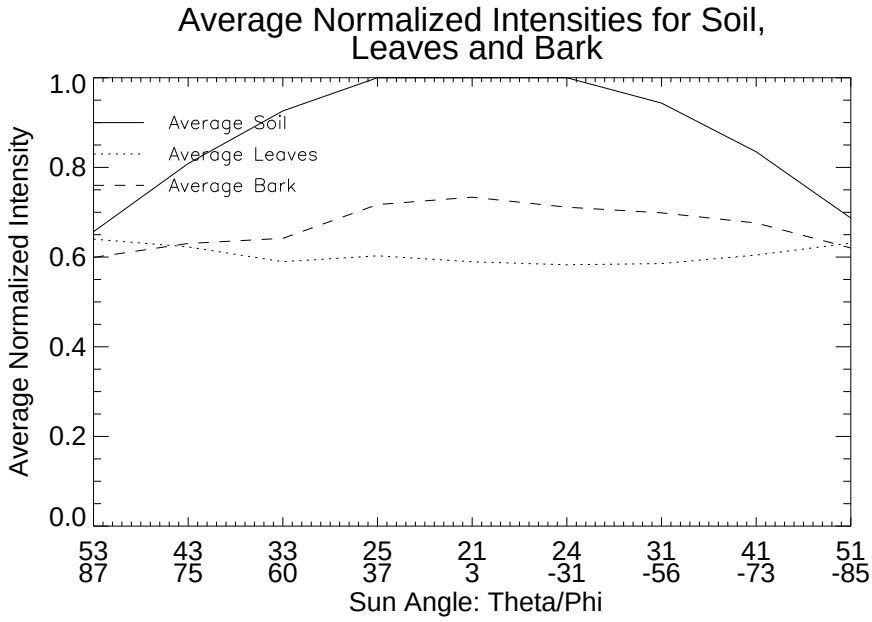

Figure 27: Average cosine of angle between the surface normal and sun vector for visible illuminated surfaces as a function of illumination directions

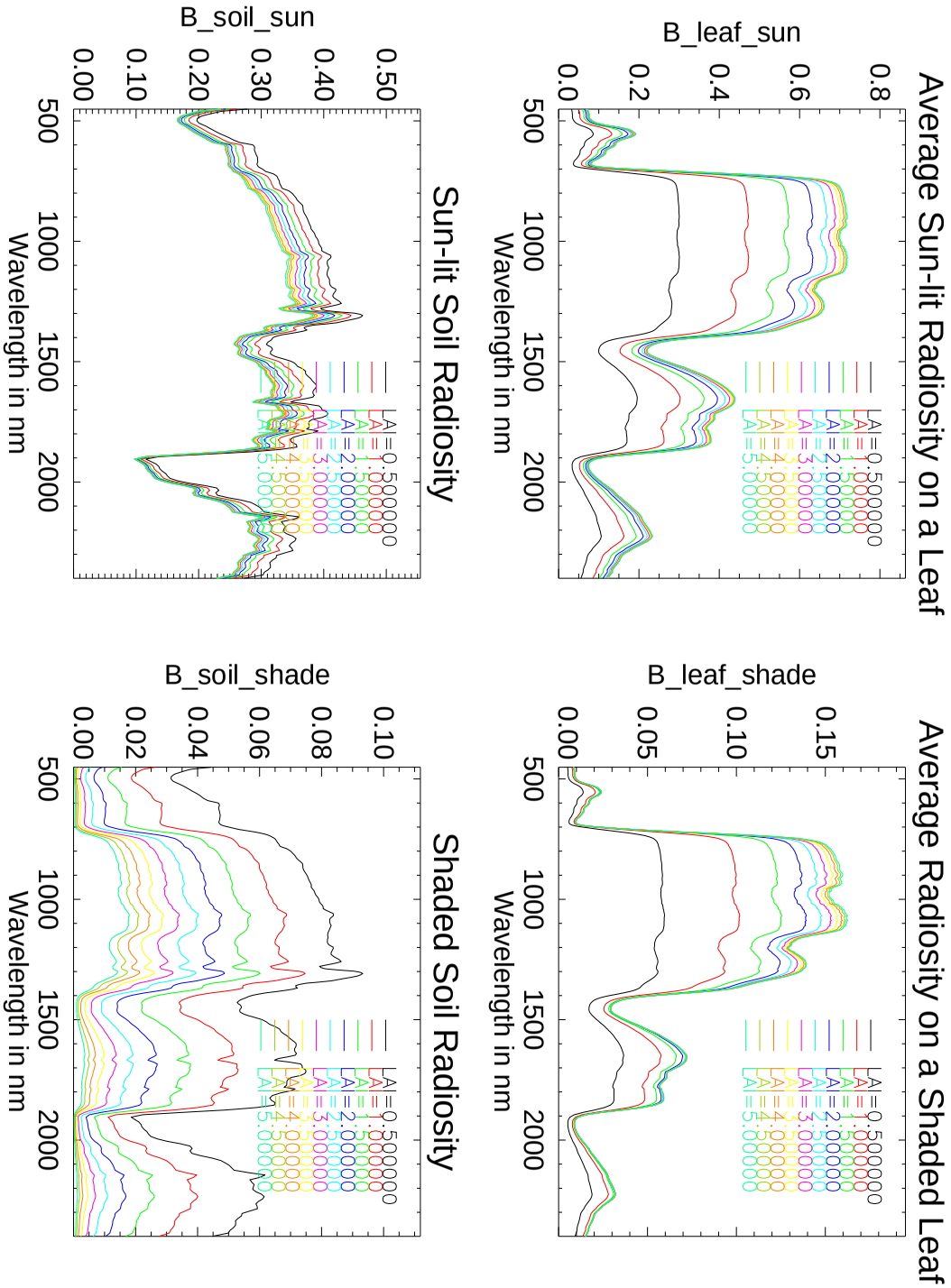

Figure 28: Canopy averaged spectra for a walnut canopy

$$f_{canopy}(\theta_v, \phi_v; \theta_s, \phi_s; \lambda) =$$

$$\frac{1}{E_0 \cos\theta_s}\Big[\, P^{sun}_{leaf}\overline{(\vec{n}_{leaf}\cdot\vec{n}_{sun})}\overline{B^{sun}_{leaf}} + P^{shade}_{leaf}\cos\theta_s\overline{B^{shade}_{leaf}}$$

$$+P^{sun}_{soil}\cos\theta_s\overline{B^{sun}_{soil}} \; + P^{shade}_{soil}\cos\theta_s\overline{B^{shade}_{soil}}\Big]$$

In Figures 29 and 30 we show the spectra over a simulated walnut canopy.

5. Plot spectral BRDF for given view/sun directions. In Fig.31 a scatterplot shows how the spectrum of a canopy differs from the reflectance spectrum of a single leaf. Note that the curves bend upwards for high leaf reflectances similar to Fig. 22. Thus for small reflectance values we can assume that the canopy BRDF is proportional to the leaf reflectance. The sun direction (θ_s, ϕ_s) changes the probabilities for seeing illuminated and shaded surfaces and the curves have loops because the leaf reflectance is not equal to the leaf transmittance.

The following statements can be made from our simulations :

- For a given view direction and varying sun angles the canopy architecture influences the probabilities of seeing illuminated surfaces and thus the spectral signature (e.g. for a location 45^0 N on June 21 between 10 am and 2pm the spectrum changes are about 20 % in the NIR (800-2400 nm) and about 25 to 35 % in the visible for an LAI=0.5,...,5).
- For a given sun angle and variable viewing directions the canopy architecture has a small influence on the spectral signature (e.g. for LAI=.5,..,5. and view angles from -40^0 to 40^0 the spectrum changes are about 15 % in the NIR and up to 40 % in the visible).

5.1 AVIRIS Data over a Walnut Orchard

We obtained AVIRIS data (Flight 920820B, Run 8, Scene 3) taken over a walnut orchard near Winters, CA, (38:31:24 N, 120:06:24 W to 38:31:04 N, 120:00:09 W) on August 20, 1992 at 8:30 pm UTC. The data was radiometrically corrected and we performed an atmospheric correction using the ATREM 1.3.1 code developed by the University of Colorado, Boulder (Gao et al, 1993). Reflectance spectra over eight selected walnut orchards were created using the Spectral Imaging Processing System (SIPS) and mean, standard deviation and min/max values were stored in ASCII files, Kruse et al (1993). Unfortunately we were not able to avoid negative reflectances in the range of 390 nm to 430 nm. The problem lies either in the calibration of AVIRIS or the atmospheric correction algorithm. An example of an AVIRIS spectra is shown in Figure 32. Note that the reflectance is much lower than in the simulated walnut spectra. The sun zenith angle was about 27 degrees. Possible reasons for this discrepancy are that, the probability of illuminated leaves was higher in the measured orchard or that the soil reflectance was different.

6 Conclusions

We found that there are some nonlinear effects that are noticeable for high leaf reflectances. We also learned from our research that the spectrum on each leaf is a very complex function of its surroundings and that highly realistic descriptions are needed to model canopy spectral effects. In this paper we have shown that it is possible to combine efficient raytracing results with results of simple radiosity calculations and produce canopy level spectral signatures. The comparison to experimental data is difficult because of problems with instrumentation, calibration and ground truth.

- Radiosity models show nonlinear spectral mixing effects due to canopy architecture, varying illumination and viewing directions, soil ,bark, etc.

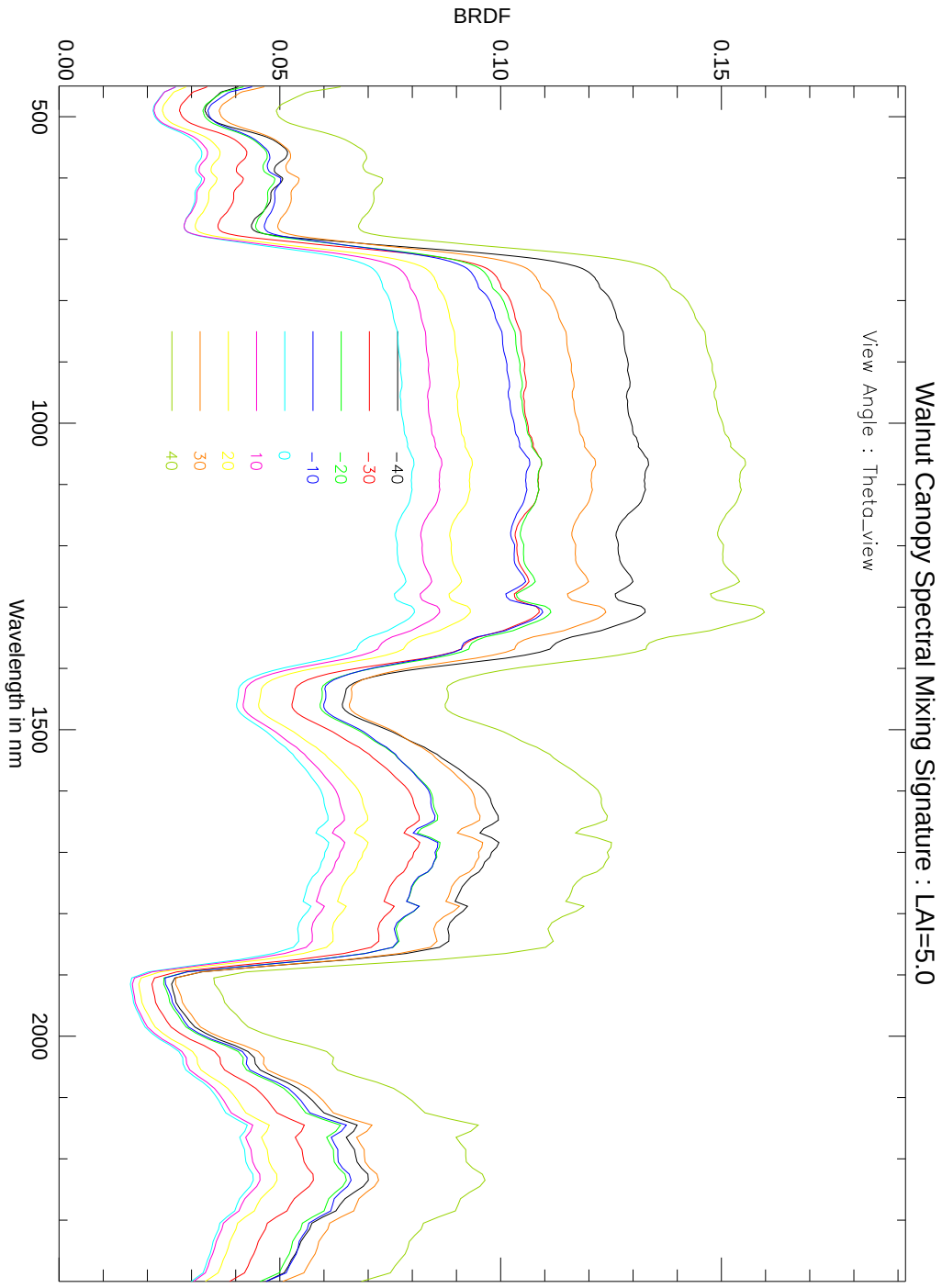

Figure 29: BRDF of a simulated walnut canopy as a function of view zenith angle

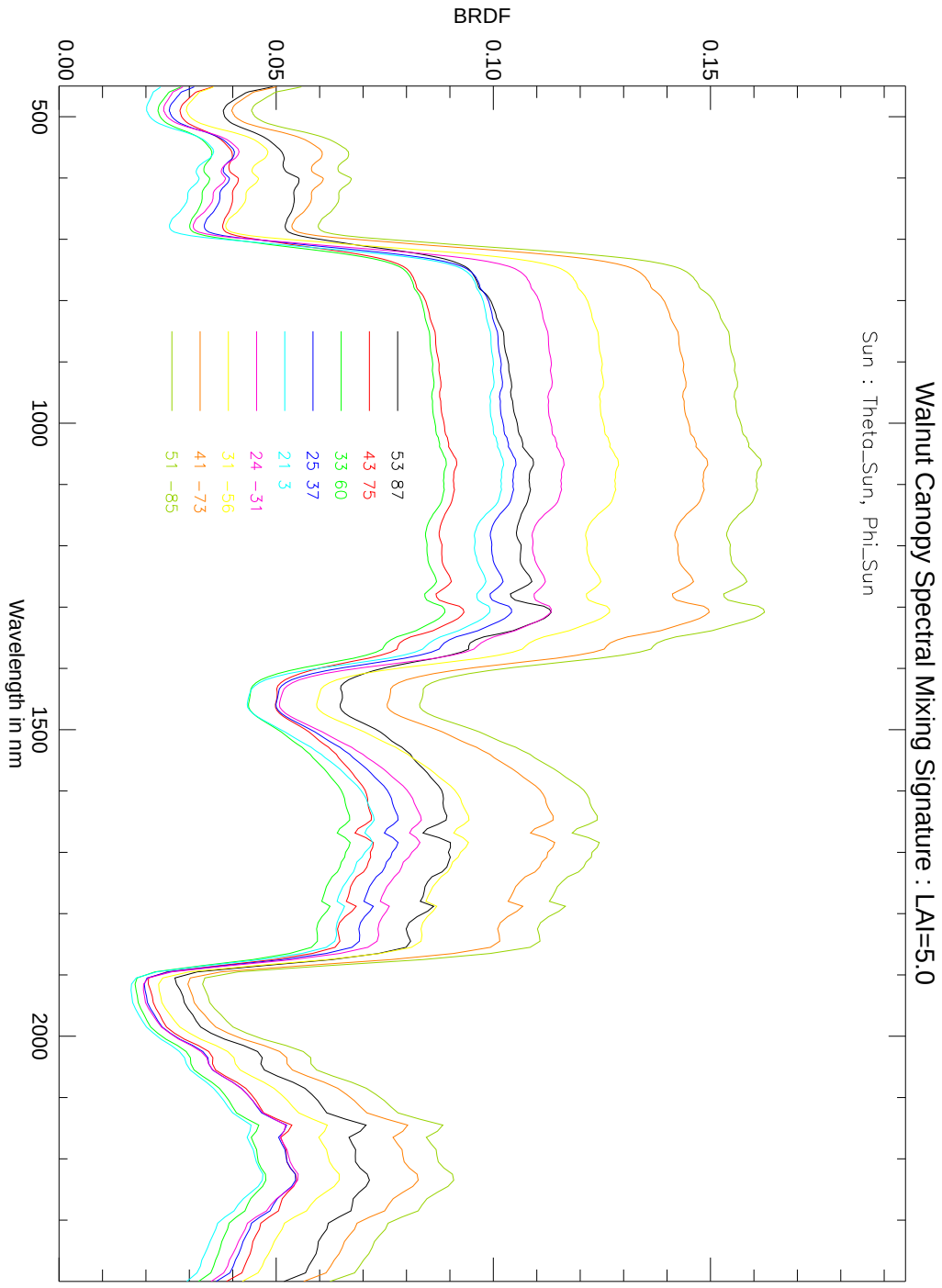

Figure 30: BRDF of a simulated walnut canopy as a function of illumination direction

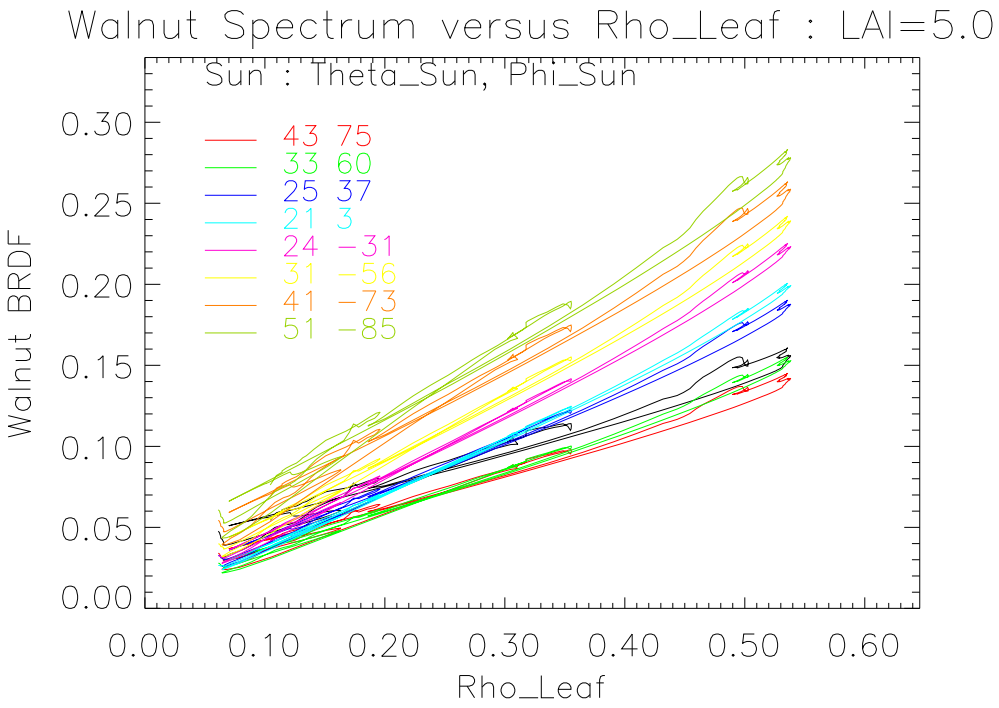

Figure 31: Canopy averaged BRDF for a walnut tree versus single leaf reflectance spectrum as a function of sun angles from 0.4 to 2.4 μm

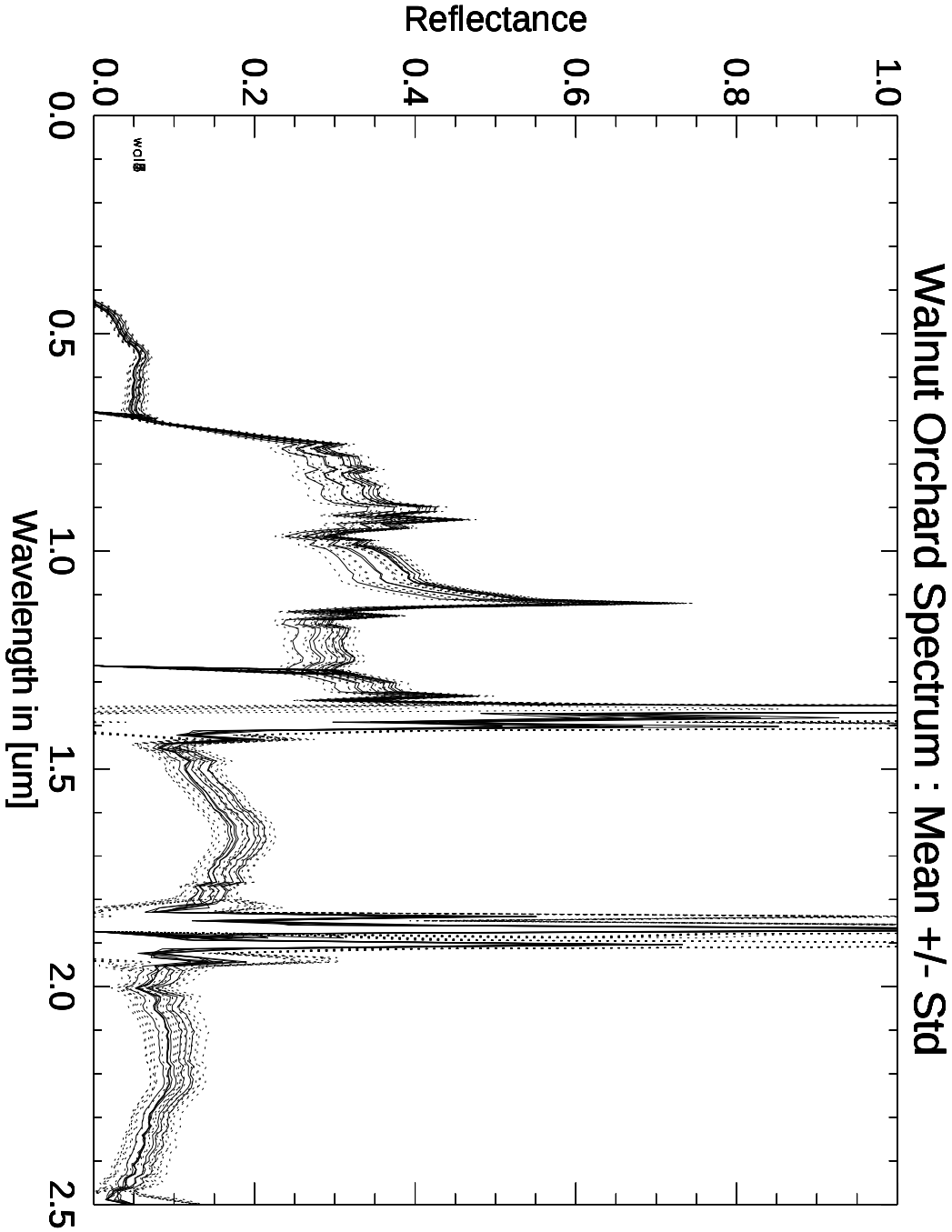

Figure 32: AVIRIS derived reflectance over a walnut orchard in Winters, CA.

- For a given view direction and varying sun angles, the canopy architecture influences the probabilities of seeing illuminated surfaces and thus the spectral signature
- For a given sun angle and variable viewing directions, the canopy architecture has a small influence on the spectral signature

Measurements and simulations show that the canopy spectrum is variable because of different amounts of multiple scattering due to clumping, specular reflections from leaves and changes in the probabilities of seeing illuminated phytoelements and background. The probabilities of seeing illuminated and shaded leaves for the model-constructed walnut tree show that over 90% of the signal comes from the canopy leaves and less than 2% from illuminated bark. Intuitively the spectral variability decreases with an increased field-of-view and this effect should be considered when experiments on miniature canopies are to be performed. More work in this area is needed to quantify the spectral variability as a function of landscape parameters, tree architecture and phytoelement size and orientation.

As the canopy becomes closed, the primary signal scattered from the canopy is from the leaves, even if the illumination and viewing angles are changed. This result, coupled with the fact that the chemical signal is derived from small absorption features spanning short wavelength intervals, provides confidence that the chemical information derived from the radiance signal is associated with leaves in a closed canopy.

7 References

D. Baum, H.E. Rushmeier, and J.M. Winget, "Improving radiosity solutions trough the use of analytically determined form-factors", *SIGGRAPH Proceedings*, 23(3):325-334, July 1989.

C.C. Borel and R.E. McIntosh, "A Backscattering model for various foliated deciduous tree types at millimeter wavelengths ", *Proc. IGARSS'86*, 8.-11 September, Zurich, Switzerland, 1986.

C.C. Borel-Donohue, *Models for Backscattering of Millimeter Waves from Vegetative Canopies*, Ph.D. Diss., Dept. of Electr. and Comp. Eng., Univ. of Massachusetts, 285 pages, 1988.

C.C. Borel, S.A.W. Gerstl and B. J. Powers. "The radiosity method in optical remote sensing of structured 3-D surfaces", *Remote Sensing of the Environment*, 36:13-44, 1991.

C.C. Borel and S.A.W. Gerstl. "Nonlinear spectral mixing models for vegetative and soil surfaces", *Remote Sensing of the Environment*, 47:403-416, 1994.

K. Cooper, J.A. Smith and D. Pitts, "Reflectance of a vegetation canopy using the adding method", *Applied Optics*, 21:4112-4118, Nov., 1982.

J.L. Dungan, L. Johnson, T. Billow, P. Matson, J. Mazzurco, J. Moen, V. Vanderbilt. "High Spectral Resolution Reflectance of Douglas Fir Grown under Differing Fertilization Regimes: Experiment Design and Treatment Effects", ACCP meeting preprint, 1994.

S.A.W. Gerstl and C.C. Borel. "Principles of the radiosity method for canopy reflectance modeling", *Proc. IGARSS'90*, 20-24 May, 3:1735-1737, 1990.

S.A.W. Gerstl and C.C. Borel. "Principals of the radiosity method versus radiative transfer for canopy reflectance modeling", IEEE Trans. on Geoscience and Remote Sensing, 30(2):271-275, 1992.

N.S. Goel, L.B Knox and J.M. Norman. "From artificial life: computer simulation of plant growth", *Int. J. General Systems*, 18:291-319.

N.S. Goel, I. Rozehnal and R.L. Thomson. "A computer graphics based model for scattering from objects of arbitrary shapes in the optical region", *Remote Sensing of the Environment*, 36:73-104, 1991.

B. Hapke, "Bidirectional reflectance spectroscopy, 1, theory", J. Geophys. Research, 86:3039-3054, 1981.

H.C. Hottel and A.F. Sarofim, *Radiative Transfer*, McGraw-Hill Book Company, New York, New York, 1967.

S. Jacquemoud and F. Baret, "PROSPECT: A model of leaf optical properties spectra", *Remote Sensing of the Environment*, 34:75-91, 1990.

S. Jacquemoud, F.Baret and J.F. Hanocq, "Modeling spectral and bidirectional soil reflectance", *Remote Sensing of the Environment*, 1992.

M.F. Jasinski, "Sensitivity of the normalized difference vegetation index to subpixel canopy cover, soil albedo, and pixel scale", *Remote Sensing of the Environment*, 32:169-187, 1990.

H.K. Lichtenthaler, "Possibilities for remote sensing of terrestrial vegetation by combination of reflectance and LASER-induced chlorophyll fluorescence", *Proc. IGARSS'89*, pp.1349-1354, 1989.

S.N. Martens, S.L. Ustin and J.M. Norman. "Measurement of tree canopy architecture", *Int. J. Remote Sensing*, 12:1525-1545, 1991.

S.N. Martens, *Modeling and Visualization of Walnut Tree Architecture*, Los Alamos Draft Report, 18 text pages with 17 figures, October 2, 1992.

G. Moschytz, *Linear Integrated Networks: Fundamentals*, Van Nostrand Reinhold, New York, 1974.

R. Schroeder, T. Hornung J. Glas, D.-U. Eisser and U. Gläser. "Three Dimensional Acoustic Digitizer", *LANL internal reports*, 1992-1993.

B. Pinty, M. Verstraete and R. Dickinson, "A physical model for predicting bidirectional reflectances over bare soil", *Rem. Sensing of the Environment*, 27:273-288, 1989.

P. Prusinkiewicz and A. Lindenmayer, *The Algorithmic Beauty of Plants*, Springer Verlag, New York, 1990.

B. Yoder, "Remote sensing of canopy chemistry at the miniature canopy scale", *Personal Communication*, Sept. 1993.

B.J. Yoder and R. E. Pettigrew-Crosby. "Predicting Nitrogen and Chlorophyll Content and Concentrations from Reflectance Spectra (400-2500 nm) at Leaf and Canopy Scales", ACCP meeting preprint, 1994.